

# Mining higher-order triadic interactions

---

Received: 12 April 2025

Accepted: 10 November 2025

---

Cite this article as: Niedostatek, M., Baptista, A., Yamamoto, J. *et al.* Mining higher-order triadic interactions. *Nat Commun* (2025). <https://doi.org/10.1038/s41467-025-66577-z>

Marta Niedostatek, Anthony Baptista, Jun Yamamoto, Jürgen Kurths, Ruben Sanchez Garcia, Ben D. MacArthur & Ginestra Bianconi

We are providing an unedited version of this manuscript to give early access to its findings. Before final publication, the manuscript will undergo further editing. Please note there may be errors present which affect the content, and all legal disclaimers apply.

If this paper is publishing under a Transparent Peer Review model then Peer Review reports will publish with the final article.

## Mining higher-order triadic interactions

Marta Niedostatek\*,<sup>1,2</sup> Anthony Baptista\*,<sup>1,2,3</sup> Jun Yamamoto,<sup>4</sup> Jürgen Kurths,<sup>5,6</sup>  
 Ruben Sanchez Garcia,<sup>2,7</sup> Ben MacArthur,<sup>2,7,8</sup> and Ginestra Bianconi<sup>1,2</sup>

<sup>1</sup>*School of Mathematical Sciences, Queen Mary University of London, London, E1 4NS, United Kingdom*

<sup>2</sup>*The Alan Turing Institute, The British Library, London, NW1 2DB, United Kingdom*

<sup>3</sup>*Cancer Bioinformatics, School of Cancer and Pharmaceutical Sciences,*

*Faculty of Life Sciences and Medicine, King's College London, London, WC2R 2LS, UK*

<sup>4</sup>*Department of Network and Data Science, Central European University, Vienna 1100, Austria*

<sup>5</sup>*Potsdam Institute for Climate Impact Research, 14473 Potsdam, Germany*

<sup>6</sup>*Institute of Physics, Humboldt University of Berlin, 12489 Berlin, Germany*

<sup>7</sup>*School of Mathematical Sciences, University of Southampton, Southampton SO17 1BJ, United Kingdom*

<sup>8</sup>*Faculty of Medicine, University of Southampton, Southampton SO17 1BJ, United Kingdom*

**Abstract** Complex systems often involve higher-order interactions that go beyond pairwise networks. Triadic interactions, where one node regulates the interaction between two others, are a fundamental form of higher-order dynamics found in many biological systems, from neuron–glia communication to gene regulation and ecosystems. However, triadic interactions have so far been mostly neglected. In this article, we propose the Triadic Perceptron Model (TPM) which shows that triadic interactions can modulate the mutual information between the dynamical states of two connected nodes. Leveraging this result, we formulate the Triadic Interaction Mining (TRIM) algorithm to extract triadic interactions from node metadata, and we apply this framework to gene expression data, finding new candidates for triadic interactions relevant for Acute Myeloid Leukemia. Our findings highlight crucial aspects of triadic interactions that are often ignored, offering a framework that can deepen our understanding of complex systems across biology, ecology, and climate science.

## INTRODUCTION

Higher-order networks [1–5] are key to capturing many-body interactions present in complex systems. Inferring higher-order interactions [6–11] from real, pairwise network datasets is recognised as one of the central challenges in the study of higher-order networks [2, 12], with wide applicability across different scientific domains, from biology and brain research [13–15] to finance [16, 17]. Mining higher-order interactions from the exclusive knowledge of the pairwise networks typically involves generative models and Bayesian approaches based on network structural properties [6, 7, 9, 11, 18]. Note, however, that when the inference is performed on the basis of the knowledge of the nodes' dynamical states [8, 10], inferring higher-order interactions also requires dynamical considerations.

Triadic interactions [19] are a fundamental type of signed higher-order interaction that are gaining increasing attention from the statistical mechanics community [19–24], since they are not reducible to hyperedges or simplices. A triadic interaction occurs when one or more nodes regulate the interaction between two other nodes. The regulator nodes may either enhance or inhibit the interaction between the other two nodes. Triadic interactions are known to be important in various systems, including: ecosystems [25–27] where one species can regulate the interaction between two other species; neuronal networks [28], where glial cells regulate synaptic trans-

mission between neurons thereby controlling brain information processing; and gene regulatory networks [29, 30], where a modulator can promote or inhibit the interaction between a transcription factor and its target gene. There is mounting evidence that triadic interactions can induce collective phenomena and/or modulate dynamical states that reveal important aspects of complex system behavior [19–24, 31, 32]. An important advance in this line of research is triadic percolation [19–21], a theoretical framework that captures the non-trivial dynamics of the giant component. Moreover, recent results demonstrate that triadic interactions can have significant effects on stochastic dynamics [24] and learning [22, 23]. However, despite the increasing attention that higher-order interactions are receiving, the detection of triadic interactions from network data and node time series, is an important scientific challenge that has not been thoroughly explored [29, 33, 34].

In this article, we formulate the Triadic Perceptron Model (TPM) in which continuous node variables are affected by triadic interactions. Based on the insights gained by investigating this model, we propose an information theoretic approach, leading to the Triadic Interaction Mining (TRIM) algorithm, for mining triadic interactions. The TPM provides evidence of the mechanisms by which a triadic interaction can induce a significant variability of the mutual information between two nodes at the end-points of an edge. The TRIM algorithm leverages this finding and mines triadic interactions using knowledge of the network structure and the dynamical variables associated with the nodes. The significance of each putative triadic interaction is then validated by comparison with two distinct null models.

\* These authors contributed equally to this work

In this way, the TRIM algorithm can go beyond monotonicity assumptions regarding the functional form of the regulation of the two linked nodes by the third node (which is at the foundation of previously proposed methods [29]) allowing for broader applications. Significant node triples are also associated with an normalized entropic score function  $S \in [0, 1]$  that quantifies the spread of the conditional joint distribution functions of the variables at the ends of the regulated edge. We test the TRIM algorithm on the benchmark TPM, demonstrating its efficiency in detecting true triadic interactions. We also use the TRIM model to mine triadic interactions from gene-expression, to identify ‘trigenic’ processes [35]. We demonstrate that the TRIM algorithm is able to detect known interactions as well as propose a set of new candidate interactions that can then be validated experimentally.

## RESULTS

### Triadic interactions

A triadic interaction occurs when one or more nodes modulate (or regulate) the interaction between two other nodes, either positively or negatively. A *triadic interaction network* is a heterogeneous network composed of a structural network and a regulatory network encoding triadic interactions (Figure 1). The *structural network*  $G_S = (V, E_S)$  is formed by a set  $V$  of  $N$  nodes and a set  $E_S$  of  $L$  edges. The *regulatory network*  $G_R = (V, E_S, E_R)$  is a signed bipartite network with one set of nodes given by  $V$  (the nodes of the structural network), and another set of nodes given by  $E_S$  (the edges of the structural network) connected by the regulatory interactions  $E_R$  of cardinality  $|E_R| = \hat{L}$ . The signed regulatory network can be encoded as an  $L \times N$  matrix  $K$  where  $K_{\ell i} = 1$  if node  $i$  activates the structural edge  $\ell$ ,  $K_{\ell i} = -1$  if node  $i$  inhibits the structural edge  $\ell$  and  $K_{\ell i} = 0$  otherwise. If  $K_{\ell i} = 1$ , then the node  $i$  is called a *positive regulator* of the edge  $\ell$ , and if  $K_{\ell i} = -1$ , then the node  $i$  is called a *negative regulator* of the edge  $\ell$ . It is worth noting that node  $i \in V$  cannot serve as both a positive and negative regulator for the same edge  $\ell$  at the same time. However, node  $i$  can act as a positive regulator for edge  $\ell$  while simultaneously functioning as a negative regulator for a different edge  $\ell' \neq \ell$ .

### The Triadic Perceptron Model (TPM)

Here, we formulate a model for node dynamics in a network with triadic interactions that we call Triadic Perceptron Model (TPM). The TPM acts as a benchmark to validate the TRIM algorithm proposed here. We assume that each node  $i$  of the network is associated with a dynamical variable  $X_i \in \mathbb{R}$ , and that the dynamical state of the entire network is encoded in the state vector

$\mathbf{X} = (X_1, X_2, \dots, X_N)^T$ . The topology of the structural network is encoded in the graph Laplacian matrix  $\mathbf{L}$  with elements

$$L_{ij} = \begin{cases} -a_{ij}J & \text{if } i \neq j, \\ \sum_k a_{ik}J & \text{if } i = j, \end{cases} \quad (1)$$

where  $\mathbf{a}$  is the adjacency matrix of the network of elements  $a_{ij}$ , and  $J > 0$  is a coupling constant. In the absence of triadic interactions, we assume that the dynamics of the network is associated with a Gaussian process implemented as the Langevin equation

$$\frac{d\mathbf{X}}{dt} = -\frac{\delta\mathcal{H}}{\delta\mathbf{X}} + \Gamma\boldsymbol{\eta}(t), \quad (2)$$

with the Hamiltonian

$$\mathcal{H} = \frac{1}{2}\mathbf{X}^\top(\mathbf{L} + \alpha\mathbf{I})\mathbf{X}, \quad (3)$$

where  $\Gamma > 0$ ,  $\alpha > 0$ , and where  $\boldsymbol{\eta}(t)$  indicates uncorrelated Gaussian noise with

$$\langle \eta_i(t) \rangle = 0, \quad \langle \eta_i(t)\eta_j(t') \rangle = \delta_{ij}\delta(t - t'), \quad (4)$$

for all  $t$  and  $t'$ . The resulting Langevin dynamics are given by

$$\frac{d\mathbf{X}}{dt} = -(\mathbf{L} + \alpha\mathbf{I})\mathbf{X} + \Gamma\boldsymbol{\eta}(t). \quad (5)$$

We remark that the Hamiltonian  $\mathcal{H}$  has a minimum for  $\mathbf{X} = \mathbf{0}$ , and its depth increases as the value of  $\alpha$  increases. In a deterministic version of the model ( $\Gamma = 0$ ), the effect of the structural interactions will not be revealed at stationarity. However, the Langevin dynamics with  $\Gamma > 0$  encode the topology on the network. Indeed, at equilibrium the correlation matrix  $C_{ij} = \mathbb{E}((X_i - \mathbb{E}(X_i))(X_j - \mathbb{E}(X_j)))$  is given by

$$C_{ij} = \frac{\Gamma^2}{2}[\mathbf{L} + \alpha\mathbf{I}]_{ij}^{-1}, \quad (6)$$

see Supplementary Information (SI) for details. In other words, from the correlation matrix it is possible to infer the Laplacian, and hence the connectivity of the network.

We now introduce triadic interactions in the TPM. As explained earlier, a triadic interaction occurs when one or more nodes modulate the interaction between another two nodes. To incorporate triadic interactions into the network dynamics, we modify the definition of the Laplacian operator present in the Langevin equation. Namely, we consider the Langevin dynamics

$$\frac{d\mathbf{X}}{dt} = -(\mathbf{L}^{(T)} + \alpha\mathbf{I})\mathbf{X} + \Gamma\boldsymbol{\eta}(t), \quad (7)$$

obtained from Eq.(2) by substituting the graph Laplacian  $\mathbf{L}$  with the *triadic Laplacian*  $\mathbf{L}^{(T)}$  whose elements are given by

$$L_{ij}^{(T)} = \begin{cases} -a_{ij}J_{ij}(\mathbf{X}) & \text{if } i \neq j, \\ \sum_{k=1}^N a_{ik}J_{ik}(\mathbf{X}) & \text{if } i = j. \end{cases} \quad (8)$$

Moreover, we assume that the coupling constants  $J_{ij}(\mathbf{X})$  are determined by a perceptron-like model that considers all the regulatory nodes of the link  $\ell = [i, j]$  and the sign of the regulatory interactions. Specifically, if  $\sum_{k=1}^N K_{\ell k} X_k \geq \hat{T}$  then we set  $J_{ij} = w^+$ ; if instead  $\sum_{k=1}^N K_{\ell k} X_k < \hat{T}$  then we set  $J_{ij} = w^-$ , with  $w_+, w_- \in \mathbb{R}_+$  and  $w_+ > w_-$ . Thus,

$$J_{ij}(\mathbf{X}) = w_- + (w_+ - w_-) \theta \left( \sum_{k=1}^N K_{\ell k} X_k - \hat{T} \right), \quad (9)$$

where  $\theta(\cdot)$  is the Heaviside function ( $\theta(x) = 1$  if  $x \geq 0$  and  $\theta(x) = 0$  if  $x < 0$ ). Note that, in the presence of triadic interactions, the stochastic differential equation (7) is not associated with any Hamiltonian, and a stationary state of the dynamics is not guaranteed, making this dynamical process significantly more complex than the original Langevin dynamics given in Eq.(2). The TPM is related to a recently proposed model that captures information propagation in multilayer networks [24], but the TPM does not make use of a multilayer representation of the data. Moreover the TPM is significantly different from models of higher-order interactions previously proposed in the context of consensus dynamics [36, 37] or contagion dynamics [38, 39]. Indeed, in our framework, triadic interactions between continuous variables are not reducible to standard higher-order interactions because they involve the modulation of the interaction between a pair of nodes. Moreover, this modulation of the interaction is not dependent on the properties of the interacting nodes and their immediate neighbors, as is the case in [36, 37] or in the machine learning attention mechanism [40]. On the contrary, the modulation of the interaction is determined by a third regulatory node (or a larger set of regulatory nodes) encoded in the regulatory network.

The TPM for continuous node dynamics in presence of triadic interactions is very general and comprehensively expresses the modulation of structural interactions by other nodes in the network. Therefore, the dynamics of TPM cannot be reduced to dynamics exclusively determined by pairwise interactions. An important problem that then arises is whether such interactions can be mined from observational data. To address this issue, we will develop a new algorithm – that we call the TRIM algorithm – to identify triadic interactions from data, and we will test its performance on the data generated from the TPM model described above.

### Mining triadic interactions with the TRIM algorithm

We propose the TRIM algorithm (see Figure 2) to mine triadic interactions among triples of nodes. To simplify the notation we will use the letters  $X, Y, Z$  to indicate both nodes as well as their corresponding dynamical variables.

Given a structural edge between nodes  $X$  and  $Y$ , our goal is to determine a confidence level for the existence of a triadic interaction involving an edge between node  $X$  and node  $Y$  with respect to a potential regulator node  $Z$ . Specifically, we aim to determine whether the node  $Z$  regulates the edge between node  $X$  and node  $Y$ , given the dynamical variables  $X, Y$  and  $Z$  associated with these nodes. To do so, given a time series associated with node  $Z$ , we first sort the  $Z$ -values, and define  $P$  bins in terms of the quantiles of  $z$ , chosen in such a way that each bin  $m_z$  comprises the same number of data points (ranging in our analyses from 30 to 100). We indicate with  $z_m$  the quantile of  $Z$  corresponding to the percentile  $m/P$ . Therefore, each bin  $m_z$  indicates data in which  $Z$  ranges in the interval  $[z_m, z_{m+1})$ . We indicate with  $\mu(x|z_m), \mu(y|z_m)$  and  $\mu(x, y|z_m)$  the probability density of the variables  $X, Y$  and the joint probability density of the variables  $X$  and  $Y$  in each  $m_z$  bin.

A triadic interaction is taken to occur when the node  $Z$  affects the strength of the interaction between the other two nodes  $X$  and  $Y$ . Consequently, our starting point is to consider the mutual information between the dynamical variables  $X$  and  $Y$  conditional to the specific value of the dynamical variable  $Z$ . We thus consider the quantity  $MIz(m) = MI(X, Y|Z = z_m)$  defined as

$$MIz(m) = \int dx \int dy \mu(x, y|z_m) \log \left( \frac{\mu(x, y|z_m)}{\mu(x|z_m)\mu(y|z_m)} \right).$$

In order to estimate this quantity, we rely on non-parametric methods based on entropy estimation from  $k$ -nearest neighbours [41–43] (see SI for details). For each triple of nodes, we visualize the mutual information  $MIz$  computed as a function of the  $m/P$ -th quantiles  $z_m$  and fit this function with a decision tree comprising  $r$  splits.

In the absence of triadic interactions, we expect  $MIz$  to be approximately constant as a function of the  $m/P$ -th quantiles  $z_m$ , while, in the presence of triadic interactions, we expect this quantity to vary significantly as a function of  $z_m$ . The discretised conditional mutual information CMI between  $X$  and  $Y$  conditioned on  $Z$  can be written as

$$CMI_{X,Y;Z} = \sum_{m=0}^{P-1} p(z_m) MIz(m) = \langle MIz \rangle, \quad (10)$$

where  $p(z_m) = 1/P$  indicates the probability that the  $Z$  value falls in the  $m_z$  bin. This quantity indicates important information about the interaction between the nodes  $X$  and  $Y$  when combined with the information coming from the mutual information MI given by

$$MI_{X,Y} = \int dx \int dy \mu(x, y) \log \left( \frac{\mu(x, y)}{\mu(x)\mu(y)} \right),$$

where  $\mu(x), \mu(y)$  are the probability density functions for  $X$  and  $Y$  and  $\mu(x, y)$  is the joint probability density functions of the variables  $X$  and  $Y$ . The conditional mutual information, however, is not sensitive to variations



in  $MIz$  and does not therefore provide the information needed to detect triadic interactions. In order to overcome this limitation, we define the following two quantities that measure how much the mutual information between  $X$  and  $Y$  conditioned on  $Z \in [z_m, z_{m+1})$  changes as  $z_m$  varies. Specifically we consider:

- (1) the standard deviation  $\Sigma$  of  $MIz$ , defined as

$$\Sigma = \sqrt{\sum_{m=0}^{P-1} p(z_m) [MIz(m) - \langle MIz \rangle]^2}; \quad (11)$$

- (2) the difference  $T$  between the maximum and average value of  $MIz$ , given by

$$T = \max_{m=0, \dots, P-1} |MIz(m) - \langle MIz \rangle|. \quad (12)$$

The quantities  $\Sigma$  and  $T$ , collectively measure the strength of the triadic interaction under question and can thus be used to mine triadic interactions in synthetic as well as in real data. In order to assess the significance of the putative triadic interaction, we compare the observed values of these variables to the results obtained with given null models. In order to determine if the observed values are significant with respect to a given null model, we compute the scores  $\Theta_\Sigma$ ,  $\Theta_T$ , given by

$$\begin{aligned} \Theta_\Sigma &= \frac{\Sigma - \mathbb{E}(\Sigma^{\text{ran}})}{\sqrt{\mathbb{E}((\Sigma^{\text{ran}})^2) - (\mathbb{E}(\Sigma^{\text{ran}}))^2}}, \\ \Theta_T &= \frac{T - \mathbb{E}(T^{\text{ran}})}{\sqrt{\mathbb{E}((T^{\text{ran}})^2) - (\mathbb{E}(T^{\text{ran}}))^2}}, \end{aligned} \quad (13)$$

and the  $p$ -values

$$p_\Sigma = \mathbb{P}(\Sigma^{\text{ran}} > \Sigma), \quad p_T = \mathbb{P}(T^{\text{ran}} > T), \quad (14)$$

Note that if we consider  $\mathcal{N}$  realizations of the null model, we cannot estimate probabilities smaller than  $1/\mathcal{N}$ . Therefore, if in our null model we observe no value of  $\Sigma^{\text{ran}}$  larger than the true data  $\Sigma$ , we set the conservative estimate  $p_\Sigma = 1/\mathcal{N}$ . A similar procedure is applied also to  $p_T$ .

To assess this significance we consider two types of null models. The first is the randomization null model obtained by shuffling the  $Z$  values, to give  $\mathcal{N}$  randomization of the data, i.e. we use surrogate data for testing [44, 45]. The second is the maximum likelihood Gaussian null model between the three nodes involved in the triple  $X, Y, Z$ . Specifically, the Gaussian null model uses the mean and covariance of the timeseries of  $X, Y$  and  $Z$  to define a multivariate normal distribution from which samples are randomly drawn, thereby providing surrogate timeseries values for the considered triple. We note that the use of these two null models allows us to identify also non-monotonic relationships between  $MIz$  and

$z$ , thereby going beyond underlying monotonic assumptions made elsewhere [46]. The first null model disrupts the temporal correlations between the timeseries of the node  $Z$  and the timeseries the two nodes  $X$  and  $Y$  at the endpoints of the considered edges. Therefore this null model is robust with respect to the presence of possible outliers in the dataset. However, this first null model may overlook confounding network effects that affect correlations between the dynamical variables. The second null model more efficiently captures correlations between the dynamical state of the three considered nodes due to network effects but is more sensitive to the presence of outliers in the data. To increase confidence, we therefore combined the insights coming from both these null models (see SI for details).

For each triple, the function  $MIz(m)$  is fitted with a decision tree with two splits. In this way, three different intervals of values of  $Z$  are identified, each corresponding to a distinct functional behavior of the correlation functions between the variables  $X$  and  $Y$ . While our method in principle allows for more than two splits of the decision tree, for illustrative purposes we have chosen two splits since this is the minimum number of splits needed to capture non-trivial functional behavior in  $MIz$ , such as non-monotonicity. In practice this choice of two splits will also be the best choice when data is limited, such as the gene expression data we will analyze in the following section.

We also further characterize significant triples by examining their normalized entropic score function  $S \in [0, 1]$ , which is used to characterize their corresponding functional behavior. Specifically, the entropic score  $S$  classifies the diversity of each of the joint distribution functions of  $X$  and  $Y$  conditioned on  $Z$  for each interval obtained through the decision tree (see Methods for details).

As we will discuss below, the algorithm performs well on data obtained from the TPM. In this case, we also observe that true triadic triples are characterized by a high entropic score  $S$ . On real data, the results obtained with the TRIM algorithm using randomized surrogate data might neglect potentially important network effects, this shortcoming is mitigated by performing an additional validation using the Gaussian null model and the entropic score  $S$  (see SI for the full pipeline of TRIM).

### Validation of the TRIM algorithm on the triadic perceptron model

In order to discuss the phenomenology of the TPM we first considered a representative network (see Figure 3) of  $N = 10$  nodes,  $L = 12$  edges and  $\hat{L} = 5$  triadic interactions (each formed by a single node regulating a single edge) on top of which we consider the TPM proposed in Sec. .

We found that data obtained from the TPM on this network shows a strong dependence of  $MIz(m_z)$  on  $m_z$

for the triples of nodes involved in triadic interactions, with greater significance for smaller values of  $\alpha$ . Figure 3 shows the difference between the  $MIz(m)$  profile of a triple that is involved in a triadic interaction compared to a triple that is not, demonstrating how triadic interactions modulate the  $MIz(m_z)$  profile.

Moreover, Figure 4 shows, for a given triadic interaction involving nodes  $X$ ,  $Y$  and  $Z$ , the joint distributions  $\mu_\delta(X, Y)$  of  $X$  and  $Y$  for each interval  $\delta$  of values  $Z$  determined by the decision tree. The results provide evidence of this interesting dynamical behavior of the triadic model in the case of a positive regulatory interaction. Note that the analysis of the form of the function  $MIz(m_z)$  also allows us to distinguish between positive and negative regulatory interactions, which are associated with an increase or a decrease in  $MIz$  for larger values of  $m_z$  respectively.

In the Supplementary Figures S1-S2, we display further examples of the function  $MIz$  for triadic triples. We observe the increased variability of the  $MIz$  functional behavior as the parameter  $\Gamma$  is raised, i.e. the noise increases.

These results confirm the main general principle on which the TRIM algorithm is based, i.e. that the conditional mutual information  $MIz$  is modulated by triadic interactions. To make this observation precise, we examined the performance of the TRIM algorithm in mining triadic interactions from synthetic data. We first considered the network shown in Figure 3, and using the score  $\Theta_\Sigma$ , we evaluated the Receiver Operating Characteristic (ROC) curve and Precision Recall (PR) curve for different values of the dynamical parameters (see Figure 5). Both the ROC curve and the PR curve (which addresses the limitations of the ROC curve for imbalanced datasets) indicate that the TRIM algorithm performs well on data produced by the TPM, with a better performance for higher values of  $\alpha$ .

For all parameter values, we noticed that false positives are more likely to involve short-range triples, i.e. triples in which the regulator node  $Z$  is close (in the structural network) to the end-points  $X$  and  $Y$  of the target edge.

These results indicate that the TRIM algorithm is effective in identifying triadic interactions in a small network generated using the TPM. To examine the scalability of this methodology we also tested the TRIM algorithm on a much larger model network. To this end, we consider a random Erdős-Renyi network of 100 nodes, and average degree  $c = 4$  to which we added 25 random triadic interactions (i.e., between randomly chosen nodes to randomly chosen edges), imposing the condition that each edge is at most regulated by a single node for simplicity. The results of this analysis are shown in Figure 6(a), in which we provide statistics for all possible node triples in the network (the majority of which are not triadic interactions). For each edge, we retained only the 5 most significant triples according to  $\Theta_\Sigma$ . By conditioning on the value of the third node, for each of these connected nodes we also record the conditional mutual information

CMI. In Figure 6, each considered triple corresponds to a point, colour coded according to the value of  $S$ . Stars indicate triples that are involved in a triadic interactions (see SI for details). True triadic interactions are found for triples with high  $\Theta_\Sigma$  while CMI span between high and intermediate values. This result confirms the very good performance of the TRIM algorithm on the data coming from the TPM.

To test the statistical robustness of the TRIM algorithm we also conducted the same analysis (i.e., on the same structural network with the same dynamical parameters) in which all triadic interactions were removed. The results of this analysis are shown in Figure 6(c). In this case, and as expected, the TRIM algorithm did not identify any statistically significant triadic interactions. This analysis indicates that the TRIM algorithm is able to identify true triadic interactions with a low false positive discovery rate (compare Figures 6(b)-(c)).

### Detecting triadic interactions in gene-expression data

Searching for triadic interactions in gene-expression is a problem of major interest in biology. For instance, understanding the extent to which a modulator promotes or inhibits the interplay between a transcription factor and its target gene is crucial for deciphering gene regulation mechanisms [29]. In order to address this question with our method, we considered a gene-expression dataset associated with Acute Myeloid Leukemia (AML), extracted from the Grand Gene Regulatory Network Database [50, 51].

Exhaustive mining of all potential triadic interactions from every putative triple of nodes in the AML dataset is computationally very demanding (it would require testing of  $> 260M$  triples) and likely, due to the sheer number of triples being tested, to result in false positives and/or interactions of less biological importance. Moreover, such a brute-force approach would not account for other sources of important biological information, such as putative interactions derived from other experimental sources. To account for such information, we therefore focused our analysis on edges between nodes associated with known biophysical interactions, as identified in the human Protein-Protein Interaction network (PPI) [50]. Because proteins function through physical and functional interactions, protein-protein interaction (PPI) networks provide a biologically meaningful framework for interpreting gene expression changes in terms of coordinated molecular mechanisms.[52, 53]. To do this, we considered the connected subgraph of the human PPI network that contains all the genes/proteins included in the AML gene expression data and their associated edges. This network, which contains 622 nodes and 42,511 edges, formed the structural network for our analysis [54]. To start, we focused on triples involving genes known to be associated with AML, in which the

end-points  $X$  and  $Y$  of the target are directly connected in the PPI network (see SI for details).

We then selected additional triples according to their positions in the PPI network's Maximum Spanning Tree (MST), which only includes 621 edges (see Figure 7). In order to focus on triples for which network effects are likely to be less pronounced, for each edge in the MST, connecting gene/protein  $X$  with gene/protein  $Y$  we considered all genes  $Z$  within a distance of 4 from both the  $X$  and  $Y$  as candidate regulatory nodes, i.e. the third node in the triple (see SI for details). For each considered triple of genes we assessed its significance using  $\Theta_\Sigma$  as the significance score, with  $P = 5$  bins, using  $\mathcal{N} = 5 \times 10^3$  realizations of the randomization null model (very similar results were obtained using  $\Theta_T$  as the significance score, see Supplementary Figures S3-S4 for a comparison).

Figure 8 shows the results of the TRIM algorithm for those triples with  $p_\Sigma < 0.001$ . Note that for each selected edge only the top 5 triples ranked according to the  $\Theta_\Sigma$  score are depicted. Squares indicate triples chosen from biologically relevant genes for AML. The triples deemed insignificant according to the Gaussian null model, are not shown here. The interested reader can see their visualization in Figure S6 of the SI. Figure 8 provide examples of conditional distributions of two illustrative triples that rank high in TRIM. Both triples show evidence of a triadic interaction: the triple in panel (b) is a member of the MST, while (c) is an example of a triple chosen from known biologically relevant genes for AML. Further example triples are shown in the SI. Interestingly, among the significant triples, we detected also triples in which the modulation of the mutual information is non-monotonic (see SI for details).

Many of the genes involved in the 50 highest ranking triples have already been linked to AML in the literature (see SI for Table S3 for a list of highly significant triples and Table S4 with links to the literature associating the involved genes with AML). In total, 84% of the top 50 Triples include at least one gene that has a known association with AML.

## DISCUSSION

This work provides a comprehensive information theory-based framework to model and mine triadic interactions directly from dynamic observations. The TPM we propose demonstrates that the presence of a triadic interaction leads to systematic variations in the mutual information between the two end nodes of the edge involved ( $X$  and  $Y$ ). Via this model we have shown that to detect triadic interactions it is necessary to go beyond standard pairwise measures, such as the mutual information. Importantly, standard higher-order statistical measures, such as the conditional mutual information, which accounts for the average effect of the third regulatory node  $Z$  on the mutual information between the target nodes  $X$  and  $Y$  are also insufficient to identify triadic in-

teractions. Our proposed approach, implemented in the TRIM algorithm, mines triadic interactions by identifying statistically significant variations in the mutual information between the two linked nodes conditioned on the third regulator node.

To demonstrate the efficacy of this algorithm we have tested and validated it on a new dynamical model (that we denote the TPM) and shown how it can identify triadic interactions in randomly generated triadic interaction networks. We also used it to mine putative triadic interactions from gene expression data, and connect the putative interactions with meaningful biology.

From the network theory point of view, this work opens new perspectives in the active field of modelling and inference of higher-order interactions and can be extended in many different directions, for instance by exploring the effect of triadic interactions on the dynamical state of nodes associated with discrete variables or including time delays in the regulation. From the biological point of view, our results may inspire further information-theoretic approaches to genetic regulatory network inference. Investigating the extent to which triadic interactions are tissue-specific, and if certain regulatory patterns are conserved across different tissues, could yield valuable insights. Our proposed approach could also be used to mine triadic interactions in other domains, such as finance or climate, where triadic interactions also have a significant role.

## METHODS

### Entropic score $S$ for significant triples

In order to identify and classify the significant triples  $[X, Y, Z]$  involving node  $X$  and  $Y$  whose interaction is modulated by node  $Z$ , we introduce an entropic score function  $S$  which characterizes how diverse the conditional joint distributions  $\mu_\delta(X, Y)$  of  $X$  and  $Y$  conditioned on  $Z$  in each of the obtained intervals  $\delta \in \{1, 2, 3\}$  are. Dividing the plane  $X, Y$  in  $P^2$  squares  $(i, j)$  (by binning  $X$  and  $Y$  in  $P$  bins each) with  $n_{ij}^{(\delta)}$  data points, we can calculate the participation ratio  $Y_2^{(\delta)}$  [55, 56]

$$Y_2^{(\delta)} = \sum_{i=1}^P \sum_{j=1}^P \left( \frac{n_{ij}^{(\delta)}}{\mathcal{N}^{(\delta)}} \right)^2, \quad (15)$$

where  $\mathcal{N}^{(\delta)} = \sum_{i=1}^P \sum_{j=1}^P n_{ij}^{(\delta)}$ . The inverse of the partition function is known to measure the effective number of square bins in which the distribution is localized. We can then introduce the normalized entropic score  $S$  as

$$S = -\frac{1}{3 \ln P^2} \sum_{\delta=1}^3 \ln Y_2^{(\delta)}. \quad (16)$$

The entropy  $S$  is low if all the conditional distributions  $\mu_\delta(X, Y)$  are very localized while it acquires large values

if all the conditional distributions are delocalized. We adopt a threshold  $S = 0.5$  in order to retain triples with  $S > 0.5$  indicating that in average the conditional distributions associated to these triples have more than  $\sqrt{P^2}$  significantly populated bins.

## DATA AVAILABILITY

The data used in this work a gene-expression dataset associated with Acute Myeloid Leukemia (AML), and the human Protein-Protein Interaction network (PPI) publicly available from the Grand Gene Regulatory Net-

work Database [50] and included together with our code in <https://github.com/anthbapt/TRIM>.

## CODE AVAILABILITY

The Python package TRIM generated in this study have been deposited in the GitHub database under accession code <https://github.com/anthbapt/TRIM>

## REFERENCES

- [1] Ginestra Bianconi. *Higher-Order Networks*. Elements in the Structure and Dynamics of Complex Networks. Cambridge University Press, Cambridge, 2021.
- [2] Federico Battiston, Enrico Amico, Alain Barrat, Ginestra Bianconi, Guilherme Ferraz de Arruda, Benedetta Franceschiello, Iacopo Iacopini, Sonia Kéfi, Vito Latora, Yamir Moreno, Micah M. Murray, Tiago P. Peixoto, Francesco Vaccarino, and Giovanni Petri. The physics of higher-order interactions in complex systems. *Nature Physics*, 17(10):1093–1098, 2021.
- [3] Federico Battiston, Giulia Cencetti, Iacopo Iacopini, Vito Latora, Maxime Lucas, Alice Patania, Jean-Gabriel Young, and Giovanni Petri. Networks beyond pairwise interactions: structure and dynamics. *Physics Reports*, 874:1–92, 2020.
- [4] Leo Torres, Ann S Blevins, Danielle Bassett, and Tina Eliassi-Rad. The why, how, and when of representations for complex systems. *SIAM Review*, 63(3):435–485, 2021.
- [5] Christian Bick, Elizabeth Gross, Heather A. Harrington, and Michael T. Schaub. What are higher-order networks?, 2022.
- [6] Jean-Gabriel Young, Giovanni Petri, and Tiago P. Peixoto. Hypergraph reconstruction from network data. *Communications Physics*, 4(1):135, 2021.
- [7] Martina Contisciani, Federico Battiston, and Caterina De Bacco. Inference of hyperedges and overlapping communities in hypergraphs. *Nature Communications*, 13(1):7229, 2022.
- [8] Federico Malizia, Alessandra Corso, Lucia Valentina Gambuzza, Giovanni Russo, Vito Latora, and Mattia Frasca. Reconstructing higher-order interactions in coupled dynamical systems. *Nature Communications*, 15(1):5184, 2024.
- [9] Federico Musciotto, Federico Battiston, and Rosario N Mantegna. Detecting informative higher-order interactions in statistically validated hypergraphs. *Communications Physics*, 4(1):218, 2021.
- [10] Robin Delabays, Giulia De Pasquale, Florian Dörfler, and Yuanzhao Zhang. Hypergraph reconstruction from dynamics. *arXiv preprint arXiv:2402.00078*, 2024.
- [11] Simon Lizotte, Jean-Gabriel Young, and Antoine Allard. Hypergraph reconstruction from uncertain pairwise observations. *Scientific Reports*, 13(1):21364, 2023.
- [12] Fernando E Rosas, Pedro AM Mediano, Andrea I Luppi, Thomas F Varley, Joseph T Lizier, Sebastiano Stramaglia, Henrik J Jensen, and Daniele Marinazzo. Disentangling high-order mechanisms and high-order behaviours in complex systems. *Nature Physics*, 18(5):476–477, 2022.
- [13] Fernando E Rosas, Pedro AM Mediano, Michael Gastpar, and Henrik J Jensen. Quantifying high-order interdependencies via multivariate extensions of the mutual information. *Physical Review E*, 100(3):032305, 2019.
- [14] Sebastiano Stramaglia, Tomas Scagliarini, Bryan C Daniels, and Daniele Marinazzo. Quantifying dynamical high-order interdependencies from the o-information: An application to neural spiking dynamics. *Frontiers in Physiology*, 11:595736, 2021.
- [15] Eckehard Olbrich, Nils Bertschinger, and Johannes Rauh. Information decomposition and synergy. *Entropy*, 17(5):3501–3517, 2015.
- [16] Guido Previde Massara, Tiziana Di Matteo, and Tomaso Aste. Network filtering for big data: Triangulated maximally filtered graph. *Journal of complex Networks*, 5(2):161–178, 2016.
- [17] Michele Tumminello, Tomaso Aste, Tiziana Di Matteo, and Rosario N Mantegna. A tool for filtering information in complex systems. *Proceedings of the National Academy of Sciences*, 102(30):10421–10426, 2005.
- [18] Anatol E Wegner and Sofia C Olhede. Nonparametric inference of higher order interaction patterns in networks. *Communications Physics*, 7(1):258, 2024.
- [19] Hanlin Sun, Filippo Radicchi, Jürgen Kurths, and Ginestra Bianconi. The dynamic nature of percolation on networks with triadic interactions. *Nature Communications*, 14(1):1308, 2023.
- [20] Ana P Millán, Hanlin Sun, Joaquín J Torres, and Ginestra Bianconi. Triadic percolation induces dynamical topological patterns in higher-order networks. *arXiv preprint arXiv:2311.14877*, 2023.
- [21] Hanlin Sun and Ginestra Bianconi. Higher-order triadic percolation on random hypergraphs. *Physical Review E*, 110(6):064315, 2024.
- [22] Lukas Herron, Pablo Sartori, and BingKan Xue. Robust retrieval of dynamic sequences through interaction modulation. *PRX Life*, 1(2):023012, 2023.

- [23] Leo Kozachkov, Jean-Jacques Slotine, and Dmitry Krotov. Neuron-astrocyte associative memory. *arXiv preprint arXiv:2311.08135*, 2023.
- [24] Giorgio Nicoletti and Daniel Maria Busiello. Information propagation in multilayer systems with higher-order interactions across timescales. *Physical Review X*, 14(2):021007, 2024.
- [25] Eyal Bairey, Eric D. Kelsic, and Roy Kishony. High-order species interactions shape ecosystem diversity. *Nature Communications*, 7(1):12285, 2016.
- [26] Jacopo Grilli, György Barabás, Matthew J. Michalska-Smith, and Stefano Allesina. Higher-order interactions stabilize dynamics in competitive network models. *Nature*, 548(7666):210–213, 2017.
- [27] Andrew D. Letten and Daniel B. Stouffer. The mechanistic basis for higher-order interactions and non-additivity in competitive communities. *Ecol Lett*, 22(3):423–436, March 2019.
- [28] Woo-Hyun Cho, Ellane Barcelon, and Sung Joong Lee. Optogenetic glia manipulation: Possibilities and future prospects. *Experimental Neurobiology*, 25(5):197–204, October 2016.
- [29] Kai Wang, Masumichi Saito, Brygida C. Bisikirska, Mariano J. Alvarez, Wei Keat Lim, Presha Rajbhandari, Qiong Shen, Ilya Nemenman, Katia Basso, Adam A. Margolin, Ulf Klein, Riccardo Dalla-Favera, and Andrea Califano. Genome-wide identification of post-translational modulators of transcription factor activity in human b cells. *Nature Biotechnology*, 27(9):829–837, 2009.
- [30] Federico M. Giorgi, Gonzalo Lopez, Jung H. Woo, Brygida Bisikirska, Andrea Califano, and Mukesh Bansal. Inferring protein modulation from gene expression data using conditional mutual information. *PLOS ONE*, 9(10):e109569, October 2014.
- [31] Jie Gao, Jianfeng Luo, Xing Li, Yihong Li, Zunguang Guo, and Xiaofeng Luo. Triadic percolation in computer virus spreading dynamics. *Chinese Physics B*, 34(2):028701, 2025.
- [32] Mateusz Iskrzyński, Aleksandra Puchalska, Aleksandra Grzelik, and Gökhan Mutlu. Pangraphs as models of higher-order interactions. *arXiv preprint arXiv:2502.10141*, 2025.
- [33] Dror Y. Kenett, Xuqing Huang, Irena Vodenska, Shlomo Havlin, and H. Eugene Stanley. Partial correlation analysis: applications for financial markets. *Quantitative Finance*, 15(4):569–578, April 2015.
- [34] Juan Zhao, Yiwei Zhou, Xiujun Zhang, and Luonan Chen. Part mutual information for quantifying direct associations in networks. *Proceedings of the National Academy of Sciences*, 113(18):5130–5135, May 2016.
- [35] Elena Kuzmin, Benjamin VanderSluis, Wen Wang, Guihong Tan, Raamesh Deshpande, Yiqun Chen, Matej Usaj, Attila Balint, Mojca Mattiazzi Usaj, Jolanda van Leeuwen, Elizabeth N. Koch, Carles Pons, Andrius J. Dagilis, Michael Prysizlak, Jason Zi Yang Wang, Julia Hanchard, Margot Riggi, Kaicong Xu, Hamed Heydari, Bryan-Joseph San Luis, Ermira Shuteriqi, Hongwei Zhu, Nydia Van Dyk, Sara Sharifpoor, Michael Costanzo, Robbie Loewith, Amy Caudy, Daniel Bolnick, Grant W. Brown, Brenda J. Andrews, Charles Boone, and Chad L. Myers. Systematic analysis of complex genetic interactions. *Science*, 360(6386):eaao1729, April 2018.
- [36] Leonie Neuhäuser, Renaud Lambiotte, and Michael T. Schaub. Consensus dynamics and opinion formation on hypergraphs. In *Higher-Order Systems*, pages 347–376. Springer, 2022.
- [37] Leonie Neuhäuser, Andrew Mellor, and Renaud Lambiotte. Multibody interactions and nonlinear consensus dynamics on networked systems. *Physical Review E*, 101(3):032310, 2020.
- [38] Iacopo Iacopini, Giovanni Petri, Alain Barrat, and Vito Latora. Simplicial models of social contagion. *Nature communications*, 10(1):2485, 2019.
- [39] Guilherme Ferraz de Arruda, Giovanni Petri, and Yamir Moreno. Social contagion models on hypergraphs. *Physical Review Research*, 2(2):023032, 2020.
- [40] Petar Veličković, Guillem Cucurull, Arantxa Casanova, Adriana Romero, Pietro Lio, and Yoshua Bengio. Graph attention networks. *arXiv preprint arXiv:1710.10903*, 2017.
- [41] Lyudmyla F Kozachenko and Nikolai N Leonenko. Sample estimate of the entropy of a random vector. *Problemy Peredachi Informatsii*, 23(2):9–16, 1987.
- [42] Alexander Kraskov, Harald Stögbauer, and Peter Grassberger. Estimating mutual information. *Physical review E*, 69(6):066138, 2004.
- [43] Brian C Ross. Mutual information between discrete and continuous data sets. *PloS one*, 9(2):e87357, 2014.
- [44] J Kurths and H Herzel. An attractor in a solar time series. *Physica D: Nonlinear Phenomena*, 25(1-3):165–172, 1987.
- [45] James Theiler, Stephen Eubank, André Longtin, Bryan Galdrikian, and J Doyne Farmer. Testing for nonlinearity in time series: the method of surrogate data. *Physica D: Nonlinear Phenomena*, 58(1-4):77–94, 1992.
- [46] Huili Wang, Sheng-Yan Lin, Fei-Fei Hu, An-Yuan Guo, and Hui Hu. The expression and regulation of hox genes and membrane proteins among different cytogenetic groups of acute myeloid leukemia. *Molecular genetics & genomic medicine*, 8:e1365, Sep 2020.
- [47] R. A. Alharbi, R. Pettengell, H. S. Pandha, and R. Morgan. The role of hox genes in normal hematopoiesis and acute leukemia. *Leukemia*, 27(5):1000–1008, 2013.
- [48] Huidong Guo, Yajing Chu, Le Wang, Xing Chen, Yang-peng Chen, Hui Cheng, Lei Zhang, Yuan Zhou, Feng-chun Yang, Tao Cheng, Mingjiang Xu, Xiaobing Zhang, Jianfeng Zhou, and Weiping Yuan. Pbx3 is essential for leukemia stem cell maintenance in mll-rearranged leukemia. *Int. J. Cancer*, 141(2):324–335, July 2017.
- [49] Ping Xiang, Xining Yang, Leo Escano, Ishpreet Dhillon, Edith Schneider, Jack Clemans-Gibbon, Wei Wei, Jasper Wong, Simon Xufeng Wang, Derek Tam, Yu Deng, Eric Yung, Gregg B. Morin, Pamela A. Hoodless, Martin Hirst, Aly Karsan, Florian Kuchenbauer, R. Keith Humphries, and Arefeh Rouhi. Elucidating the importance and regulation of key enhancers for human meis1 expression. *Leukemia*, 36(8):1980–1989, 2022.
- [50] Marouen Ben Guebila, Camila M Lopes-Ramos, Deborah Weighill, Abhijeet Rajendra Sonawane, Rebekka Burkholz, Behrouz Shamsaei, John Platig, Kimberly Glass, Marieke L Kuijjer, and John Quackenbush. "grand gene regulatory network database", 2023.
- [51] Marouen Ben Guebila, Camila M. Lopes-Ramos, Deborah Weighill, Abhijeet Rajendra Sonawane, Rebekka Burkholz, Behrouz Shamsaei, John Platig, Kimberly Glass, Marieke L. Kuijjer, and John Quackenbush.



Grand: a database of gene regulatory network models across human conditions. *Nucleic Acids Res*, 50(D1):D610–D621, January 2022.

- [52] Nahid Safari-Alighiarloo, Mohammad Taghizadeh, Mostafa Rezaei-Tavirani, Bahram Goliaei, and Ali Asghar Peyvandi. Protein-protein interaction networks (ppi) and complex diseases. *Gastroenterology and Hepatology from bed to bench*, 7(1):17, 2014.
- [53] Tuba Sevimglu and Kazim Yalcin Arga. The role of protein interaction networks in systems biomedicine. *Computational and structural biotechnology journal*, 11(18):22–27, 2014.
- [54] Andrei Grigoriev. A relationship between gene expression and protein interactions on the proteome scale: analysis of the bacteriophage t7 and the yeast *saccharomyces cerevisiae*. *Nucleic Acids Res.*, 29(17):3513–3519, 2001.
- [55] Marc Barthelemy, Bernard Gondran, and Eric Guichard. Spatial structure of the internet traffic. *Physica A: statistical mechanics and its applications*, 319:633–642, 2003.
- [56] Bernard Derrida and H Flyvbjerg. Statistical properties of randomly broken objects and of multivalley structures in disordered systems. *Journal of Physics A: Mathematical and General*, 20(15):5273, 1987.

#### ACKNOWLEDGMENTS

This work was sponsored by the Turing-Roche Strategic Partnership. M.N. was funded by the

UKRI/BBSRC Collaborative Training Partnership in AI for Drug Discovery and Queen Mary University of London. This research utilized Queen Mary’s Apocrita HPC facility, supported by QMUL Research-IT, <https://doi.org/10.5281/zenodo.438045>.

#### AUTHOR CONTRIBUTION STATEMENT

G.B. designed the research, M.N., A.B. and J.Y. conducted the numerical analysis, M.N., A.B. and J.Y. wrote the codes, M.N. finalized the figures, M.N., A.B., J.Y., J.K., R.S.G., B.M. and G. B. conducted the research, and wrote the paper.

#### COMPETING INTEREST STATEMENT

The authors declare no competing interests.

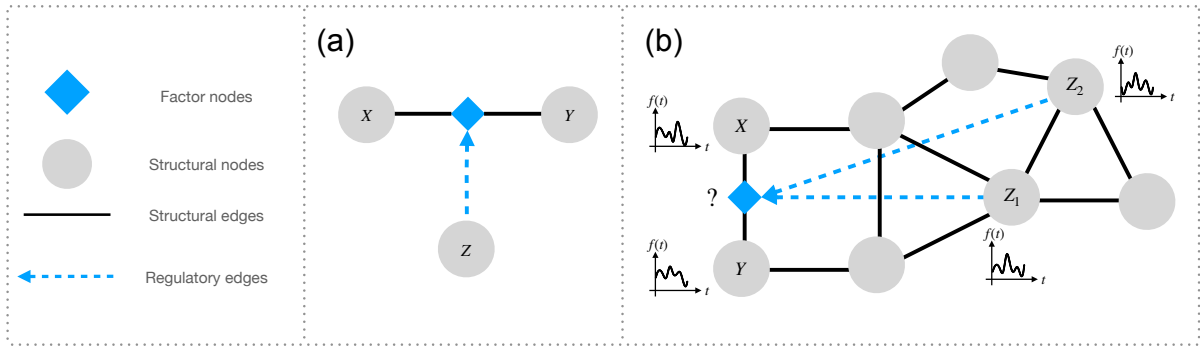


Figure 1. Schematic representation of triadic interactions. (Panel a) A triadic interaction occurs when a node  $Z$ , called a *regulator node*, regulates (either positively or negatively) the interaction between two other nodes  $X$  and  $Y$ . The regulated edge can be conceptualized as a *factor node* (shown here as a cyan diamond). (Panel b) A network with triadic interactions can be seen as a network of networks formed by a simple structural network and by a bipartite regulatory network between regulator nodes and regulated edges (factor nodes).

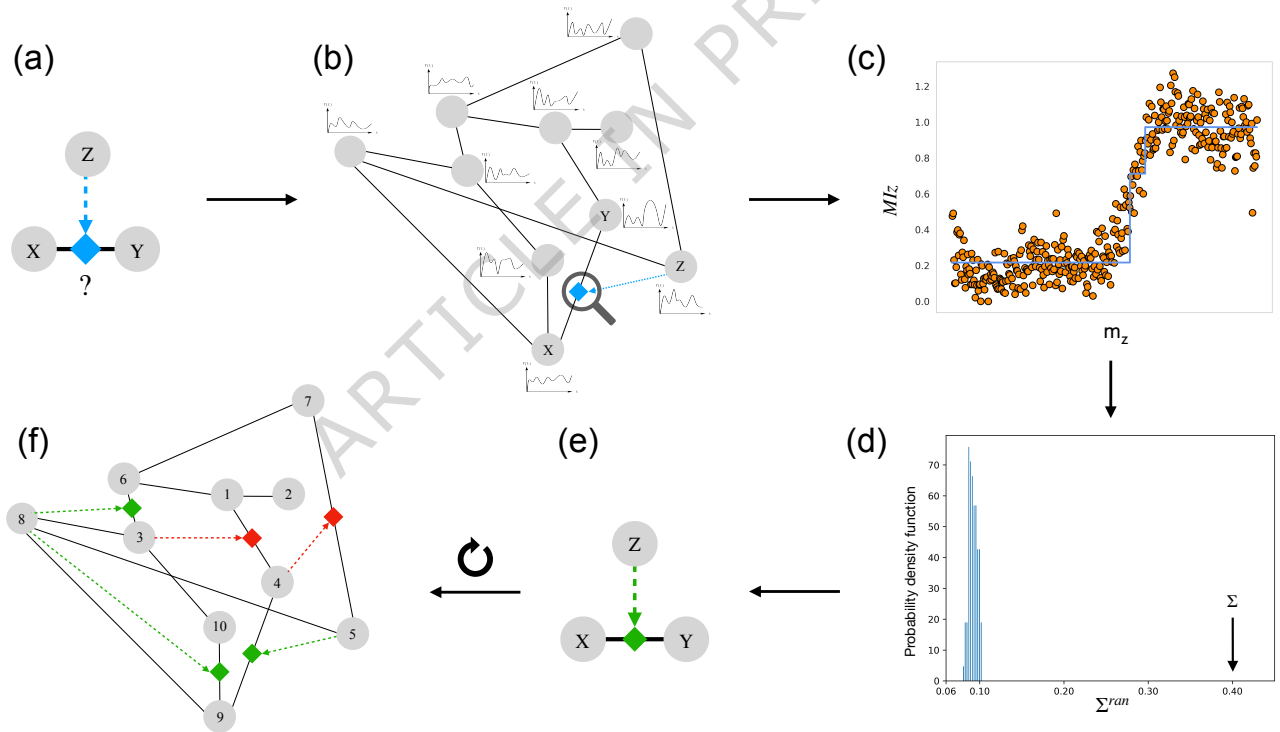


Figure 2. Illustration of the TRIM algorithm. The TRIM algorithm identifies triples of nodes  $X$ ,  $Y$ , and  $Z$  involved in a putative triadic interaction, starting from the knowledge of the structural network and the dynamical variables associated with its nodes. For each putative triple of nodes involved in a triadic interaction (panel (a)) which belong to a network whose structure and dynamics is known (panel (b)), we study the functional behavior of the conditional mutual information  $MIz$  (panel (c)), and assess the significance of the observed modulations of  $MIz$  with respect to a null model (panel (d)). Given a predetermined confidence level, we can use these statistics to identify significant triadic interactions (panel (e)). This procedure can be extended to different triples of the network, thereby identifying the triadic interactions present in it (panel (f)).

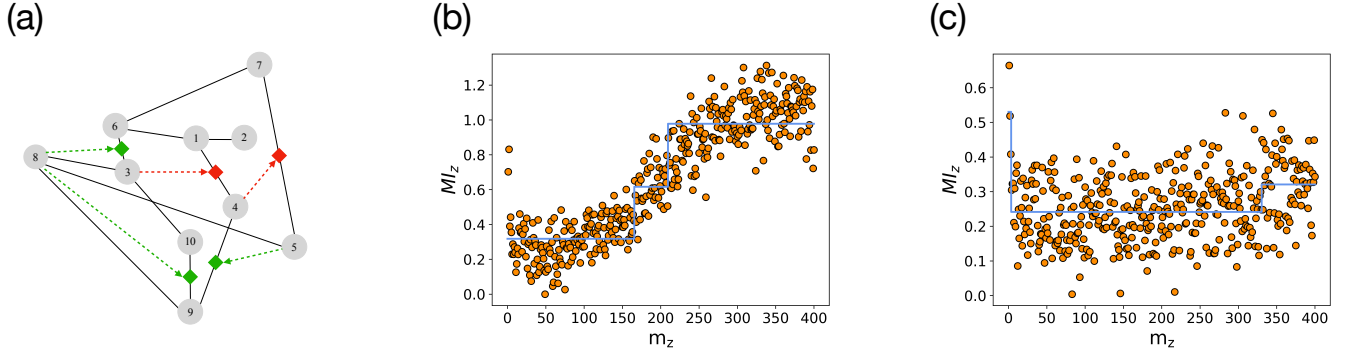


Figure 3. Illustration of the role of triadic interactions in modulating the mutual information between linked nodes. We consider a network with  $N = 10$  nodes,  $L = 12$  edges, and  $\hat{L} = 5$  triadic interactions (panel (a)). Panels (b) and (c) display the effect of triadic interactions on the Mutual Information profile  $MI_z$ . Panel (b) shows  $MI_z$  for the triple [4, 9, 5] involved in a positive triadic interaction. Panel (c) shows  $MI_z$  for the triple [1, 2, 6] that is not involved in a triadic interaction. In all panels simulations were run to  $t_{\max} = 4,000$  with a timestep of  $dt = 10^{-2}$ . For the analysis we consider 40,000 time steps. The parameters of the model are:  $\alpha = 0.05$ ,  $\hat{T} = 10^{-3}$ ,  $\Gamma = 10^{-2}$ ,  $w^+ = 8$ ,  $w^- = 0.5$ , number of bins  $P = 400$ .

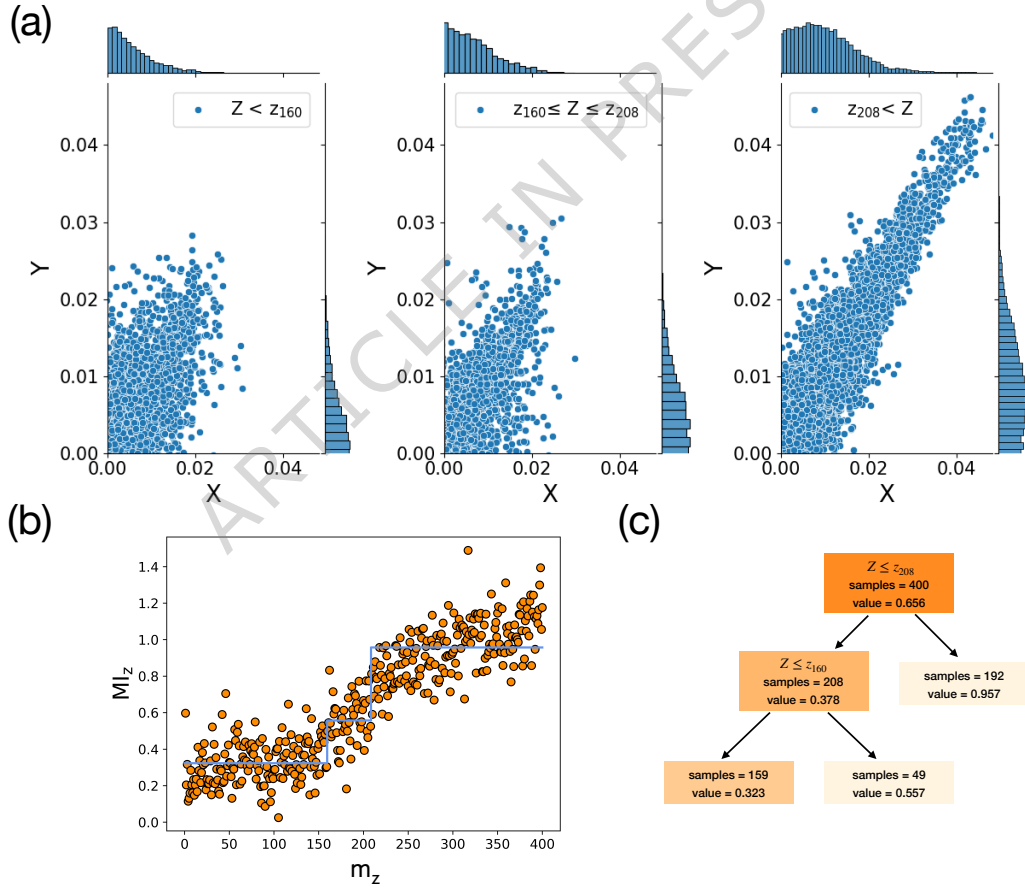


Figure 4. Representative results for triples of nodes involved in triadic interactions in the continuous model with triadic interactions. Results for the triple [4, 9, 5] of the network in Figure 3 of the main text, which is triadic, are shown. The joint distributions of variables  $X$  and  $Y$  conditional on the values of  $Z$  are shown in panel (a). Panel (b) shows the behavior of  $MI_z$  as a function of the values of  $z_m$ , which clearly departs from the constant behavior expected in absence of triadic interactions. Panel (c) presents the decision tree for fitting the  $MI_z$  functional behavior and determining the range of values of  $Z$  for which the most significant differences among the joint distributions of the variables  $X$  and  $Y$  conditioned on  $Z$  are observed. The parameters used are the same as in Figure 3.

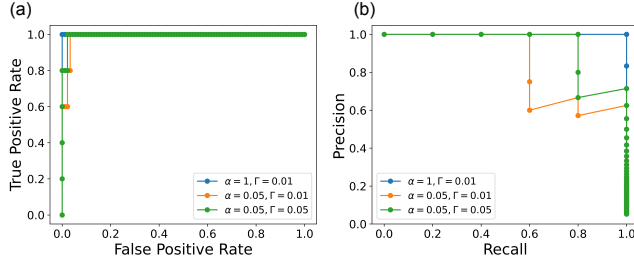


Figure 5. The performance of the TRIM algorithm on the test bench network of 10 nodes. We consider the network in Figure 3(a). The time series obtained by integrating the stochastic dynamics of the proposed dynamical model for triadic interactions (Eq.(7)) are analyzed with the TRIM algorithm. Panel (a) displays the Receiver Operating Characteristic curve (ROC curve) obtained by running TRIM with  $P = 400$  bins and  $\mathcal{N} = 10^3$  realizations of the null model on these synthetic time series, using  $\Theta_{\Sigma}$  to score for different parameters values indicated in the legend. Panel (b) displays the corresponding Precision-Recall curve (PR curve) obtained by running TRIM with the same parameters. The timeseries are simulated up to a maximum time  $t_{max} = 4000$  with a  $dt = 10^{-2}$ . For the analysis, we consider 40,000 time steps (see the SI for details). The parameter of the model are:  $\hat{T} = 10^{-3}$ ,  $w^+ = 8$ ,  $w^- = 0.5$ , and  $\alpha$  and  $\Gamma$  as indicated in the figure legend.

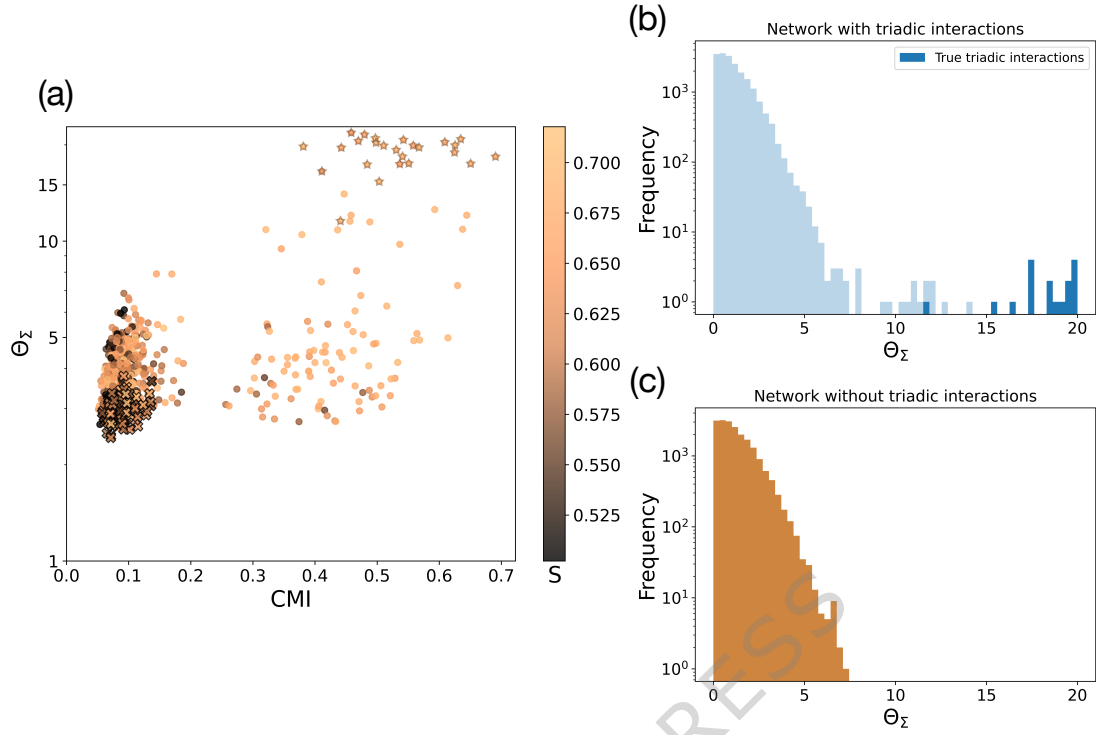


Figure 6. Performance of the TRIM algorithm on a random network with triadic interactions with  $N = 100$  nodes. (a) Each data point represents a given triple of nodes  $X$ ,  $Y$  and  $Z$ . The  $y$ -axis shows  $\Theta_\Sigma$ , while the  $x$ -axis shows the CMI between  $X$  and  $Y$ . The colour of each point corresponds to the value of  $S$ , which characterizes the entropic score of the triple. The synthetic data comes from a structural random Erdős-Renyi network with 100 nodes, and average degree  $c = 4$ , to which 25 triadic interactions between random edges and random nodes have been added. For the modelling of the network we used  $\alpha = 0.06, \Gamma = 1.4 \times 10^{-2}, t_{max} = 1500, w_+ = 18, w_- = 0.2$  and for the analysis with TRIM we looked at 3000 data points and  $P = 100$  bins. We display top 5 triples for each edge according to  $\Theta_\Sigma$  that are below our  $p$  threshold for the randomization null model. The Triples below are represented in the scatter plot and they all display an entropic score  $S > 0.5$ . Stars are the true triadic triples which are characterized by high  $\Theta_\Sigma$ . Crosses are the triples that can be excluded by performing TRIM with the Gaussian Null model. (b) Histogram of the  $\Theta_\Sigma$ -values for all the triples of the network (in light blue), and for the triples corresponding to the 25 true triadic interactions only (in dark blue). (c) Histogram of the  $\Theta_\Sigma$ -values observed in a network of the same topology and with the same dynamical parameters for which all the triadic interactions have been removed (orange).



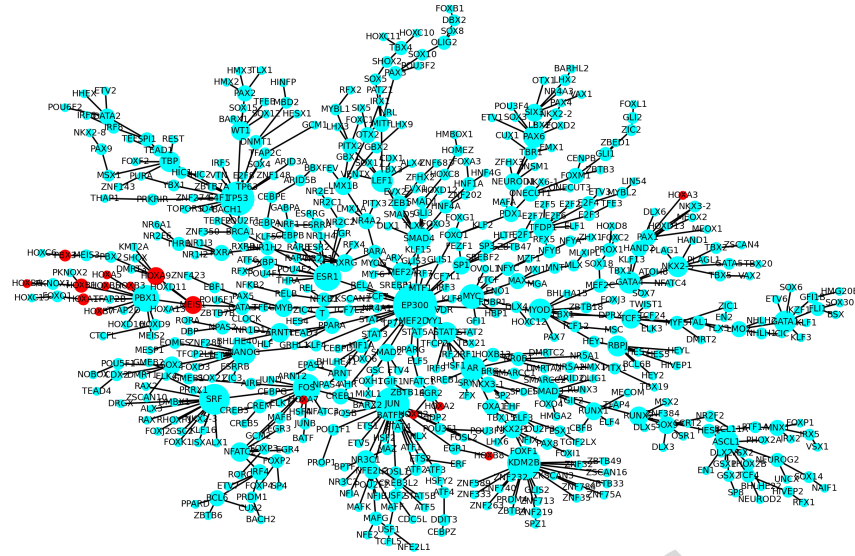


Figure 7. Maximal Spanning Tree of the relevant genes from the gene expression data. Edges and their edge weights were obtained from the Protein-Protein interaction network. Red-coloured nodes are nodes with biological significance, that is that play a critical role in AML [47–49]. Node size is proportional to the node degree.

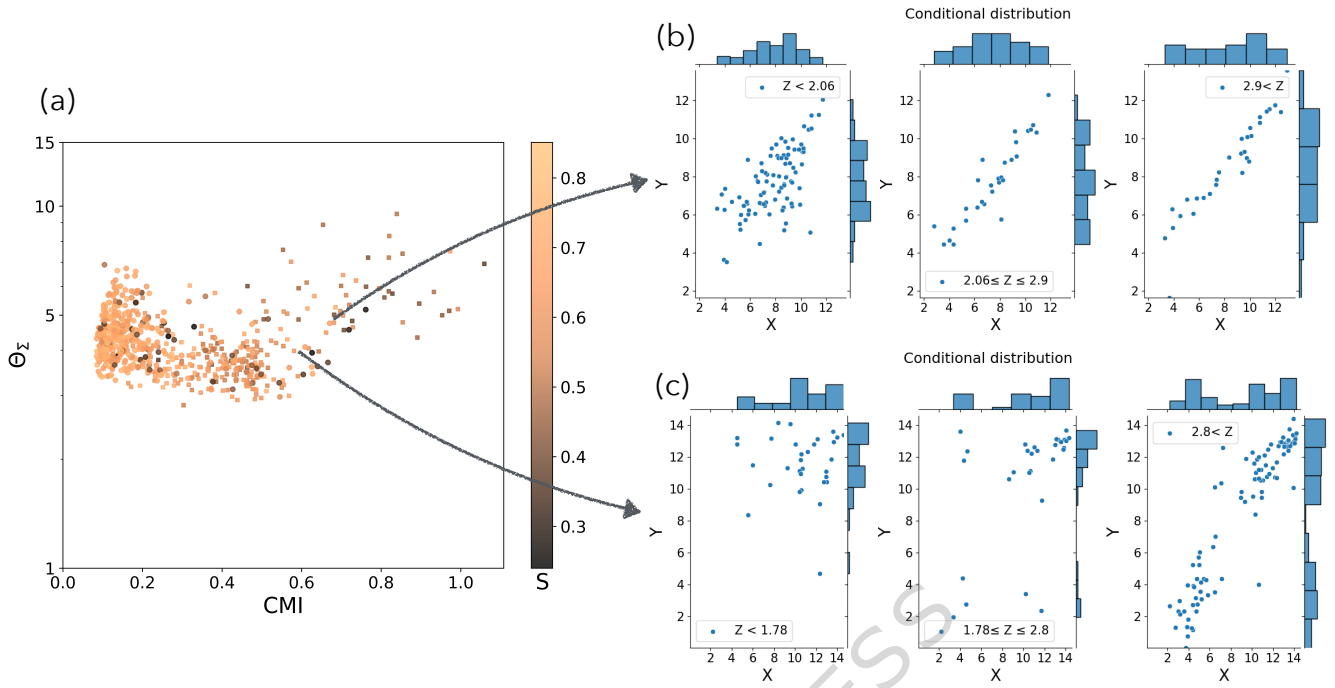
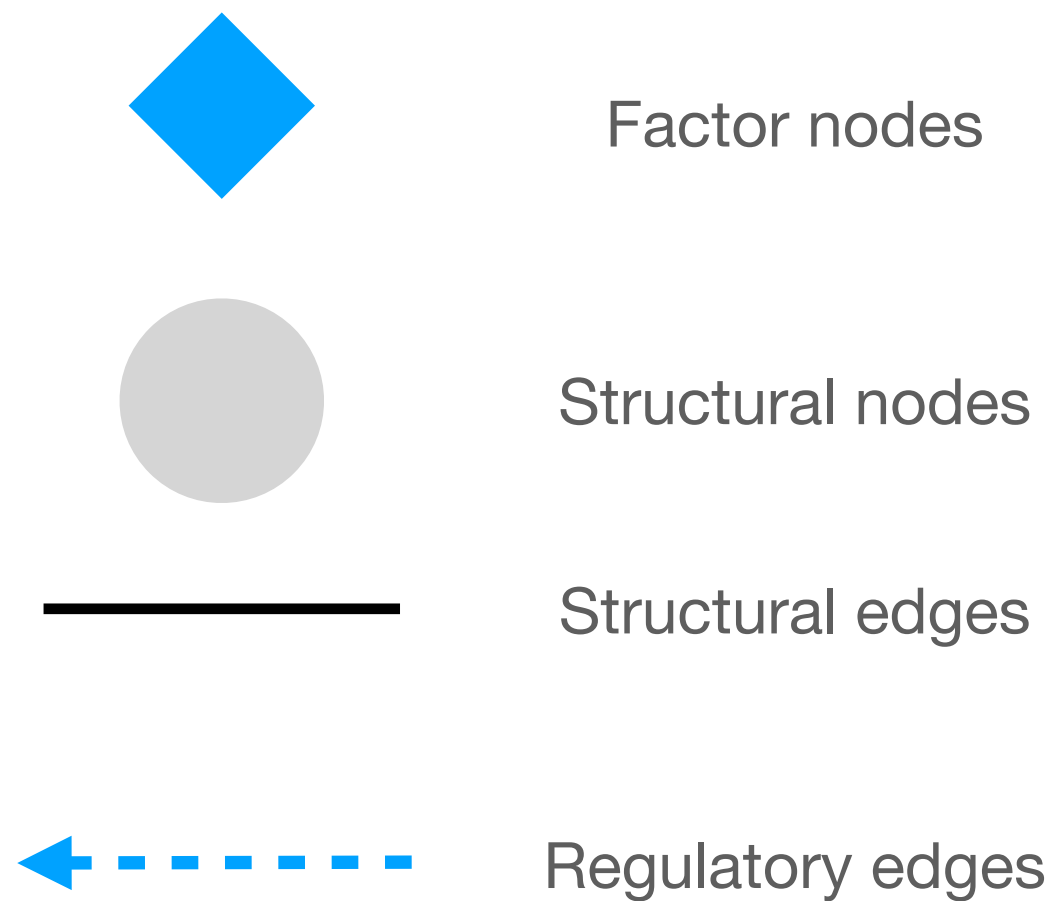
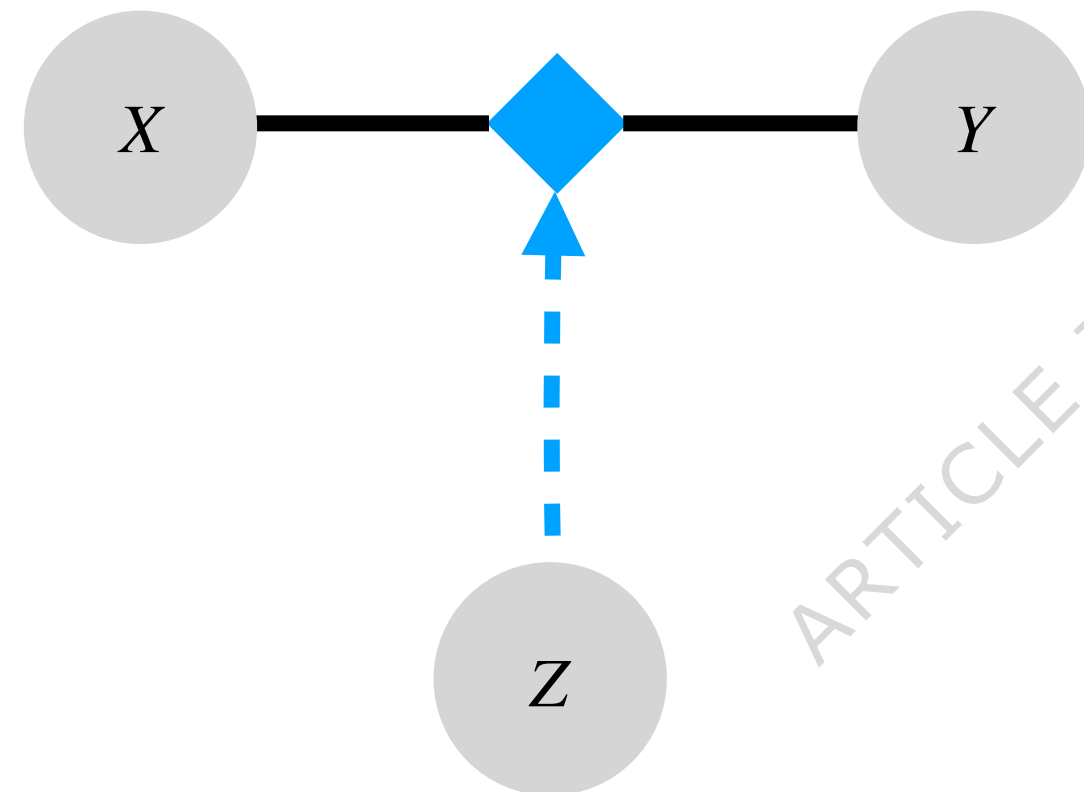


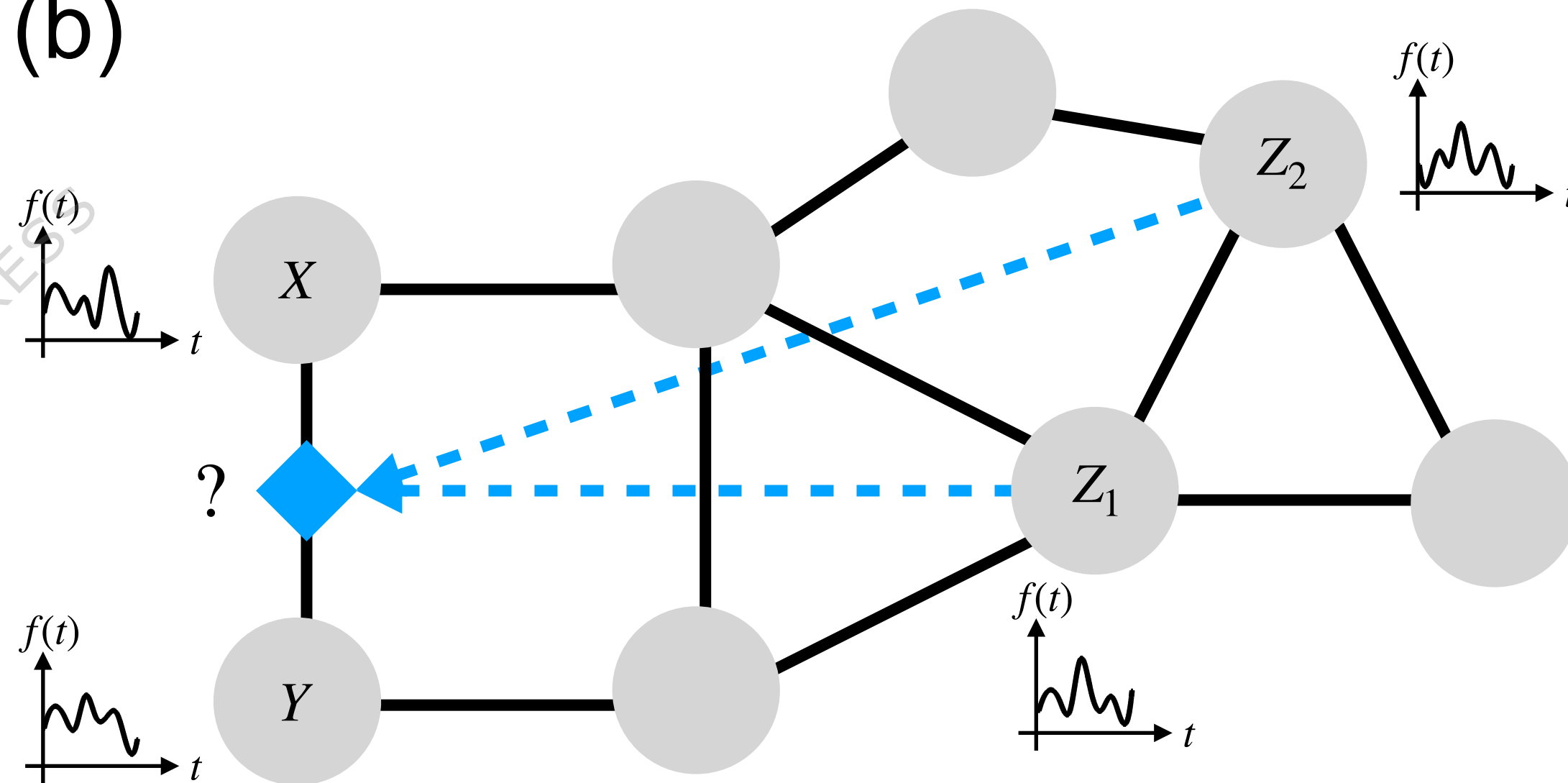
Figure 8. Application of the TRIM algorithm to gene expression data. Panel (a) shows the results of TRIM for the significant triples in the AML dataset. The scatter plot shows  $\Theta_\Sigma$  ( $y$ -axis) versus the CMI ( $x$ -axis). The colour of each point corresponds to the value of its entropic score  $S$ . Here we display only those triples with  $p$ -value 0.001 or less in the randomization null model and that have not been excluded by the Gaussian null model (for details about these triples see SI). Circles are triples whose links all appear in the minimum spanning tree, and squares indicate triples involving genes with biological relevance. Panels (b)-(c) display the conditional distributions for two example triples: both are identified by the TRIM algorithm with high significance, suggesting a meaningful biological association. Panel (b) shows the triple  $X = GATA1, Y = KLF1, Z = ETV1$ . According to the randomized surrogate null model, this triadic interaction has  $p_\Sigma$ -value 0.001,  $\Theta_\Sigma = 4.75$ ,  $\Sigma = 0.44$ ,  $S = 0.64$ ; panel (c) shows the results for the triple  $X = HOXB3, Y = MEIS1, Z = GLIS3$  involving two biologically relevant genes. According to the randomized surrogate null model, it has  $\Theta_\Sigma = 3.98$ ,  $p_\Sigma = 0.001$ ,  $\Sigma = 0.38$ ,  $S = 0.60$ .

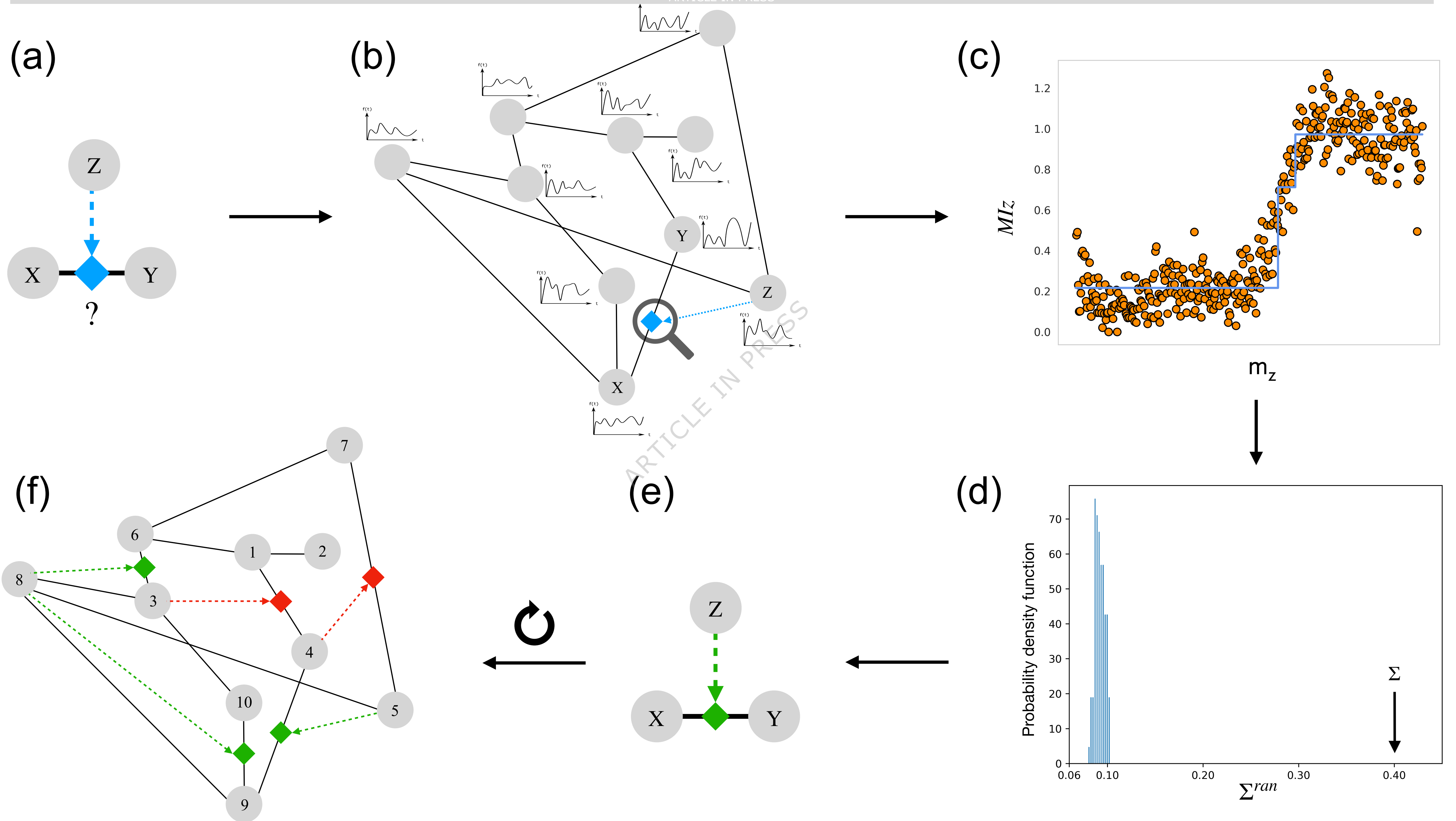


(a)

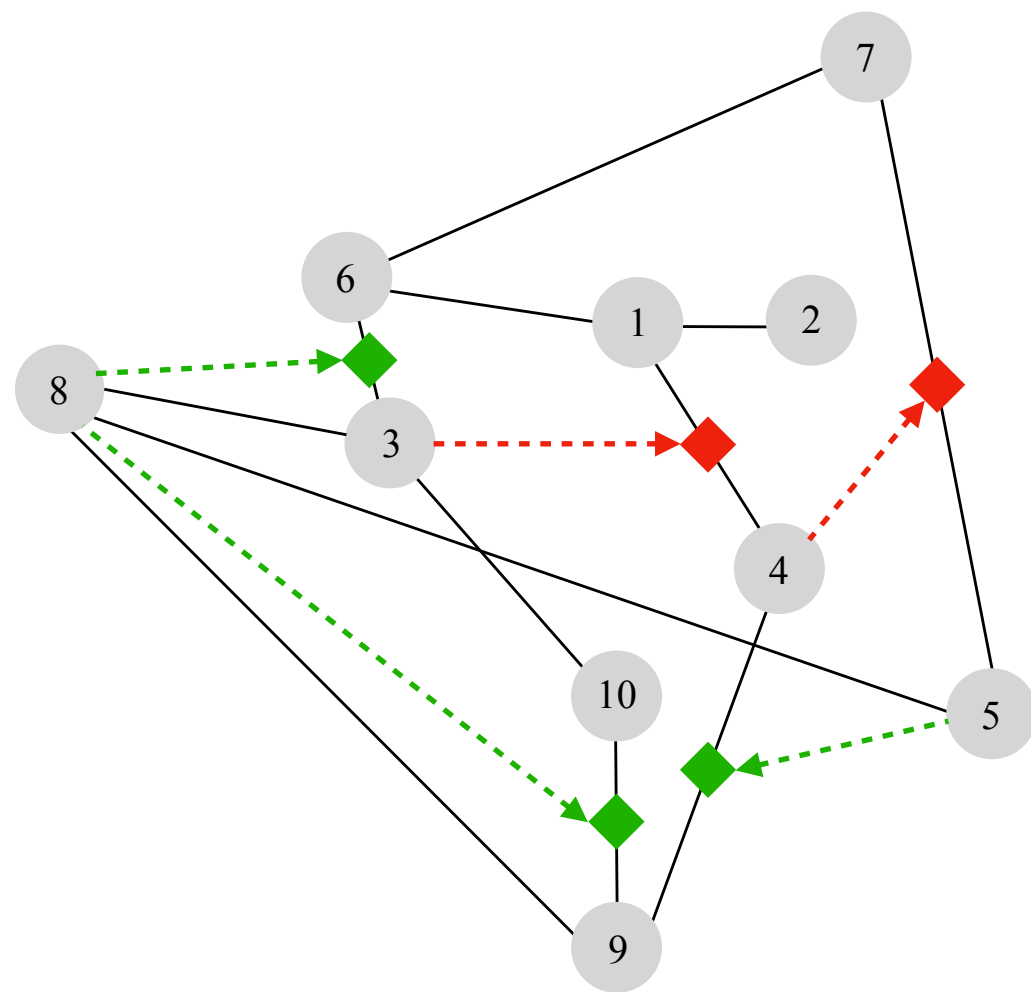


(b)

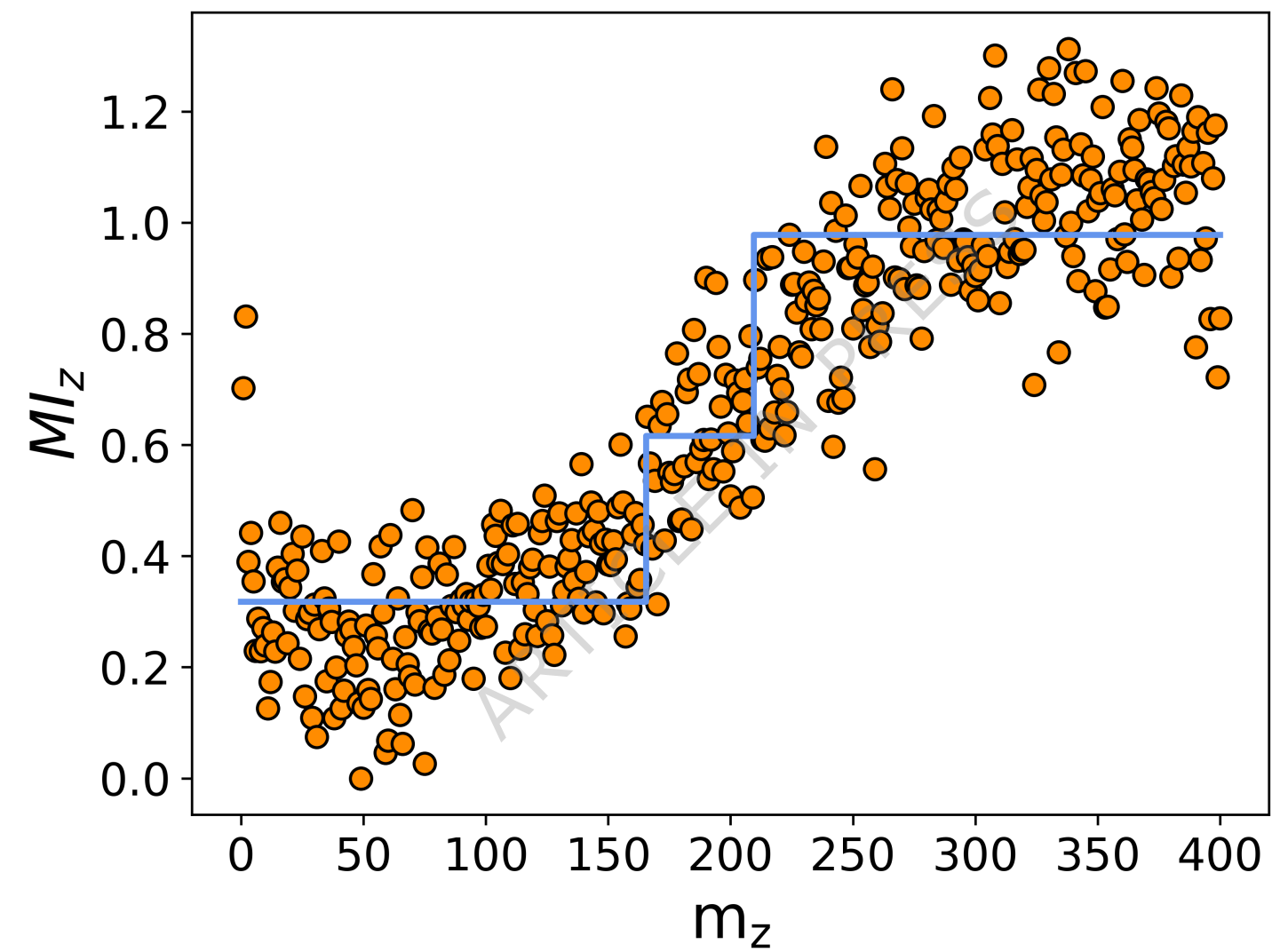




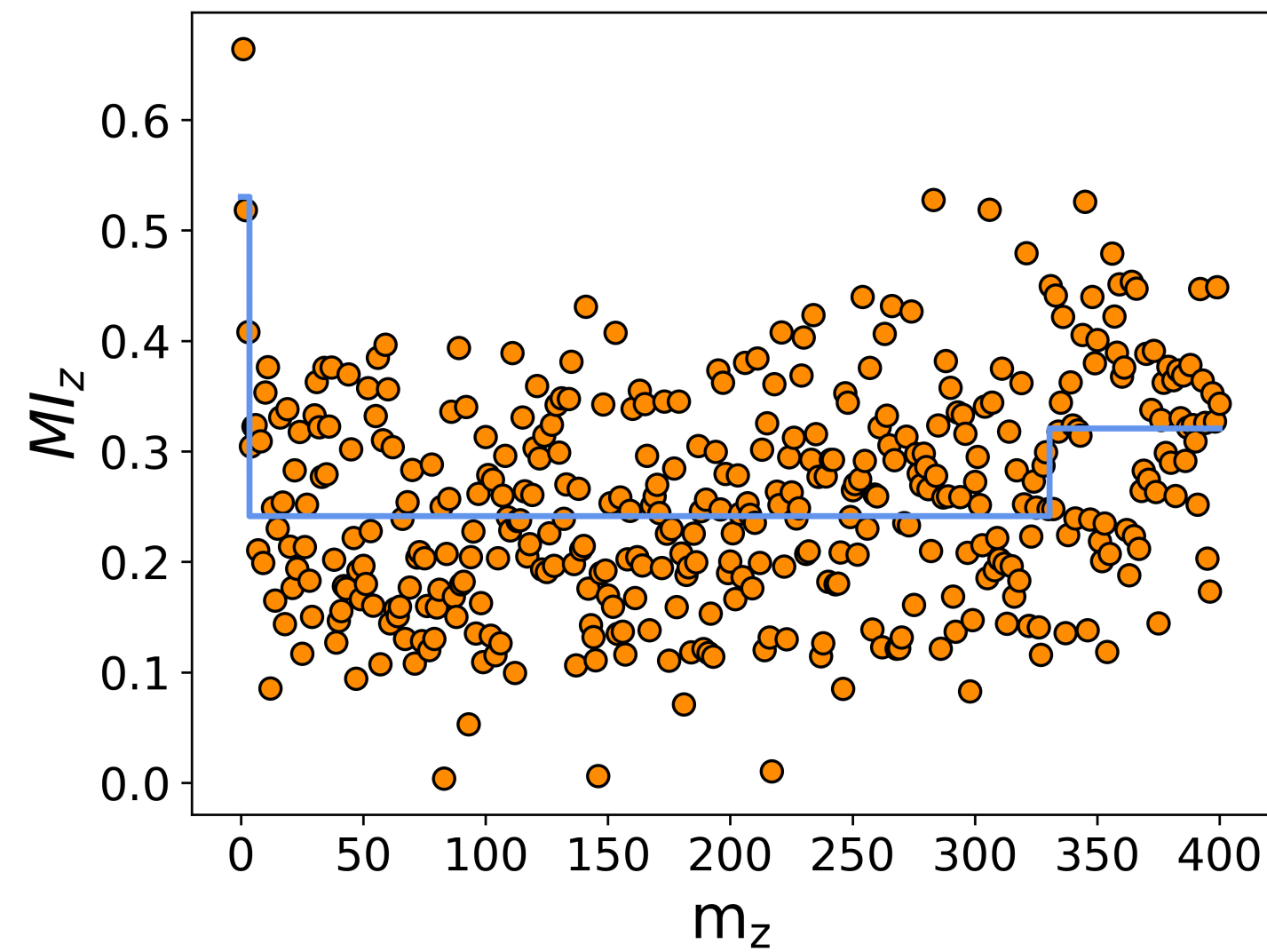
(a)



(b)

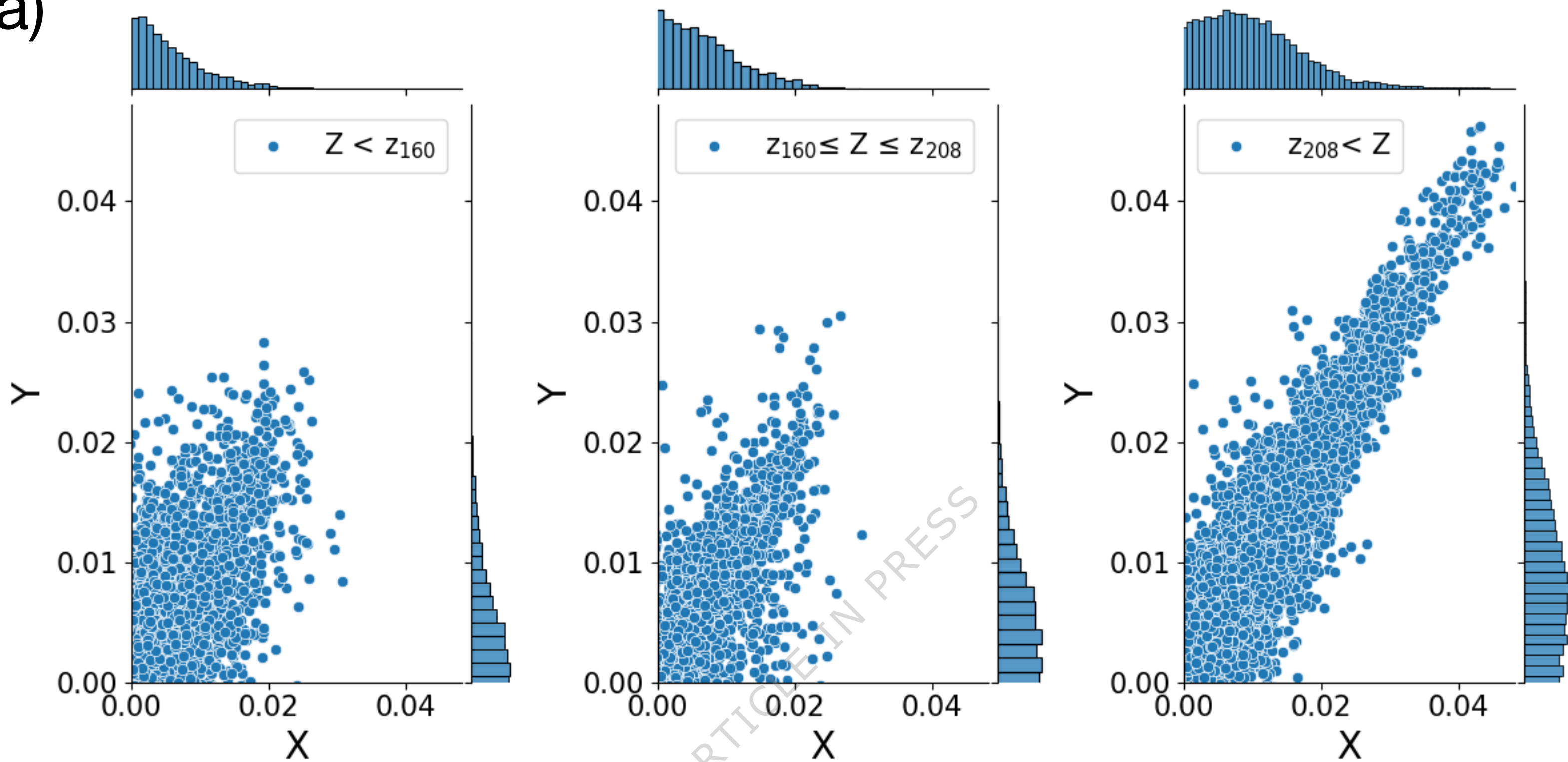


(c)

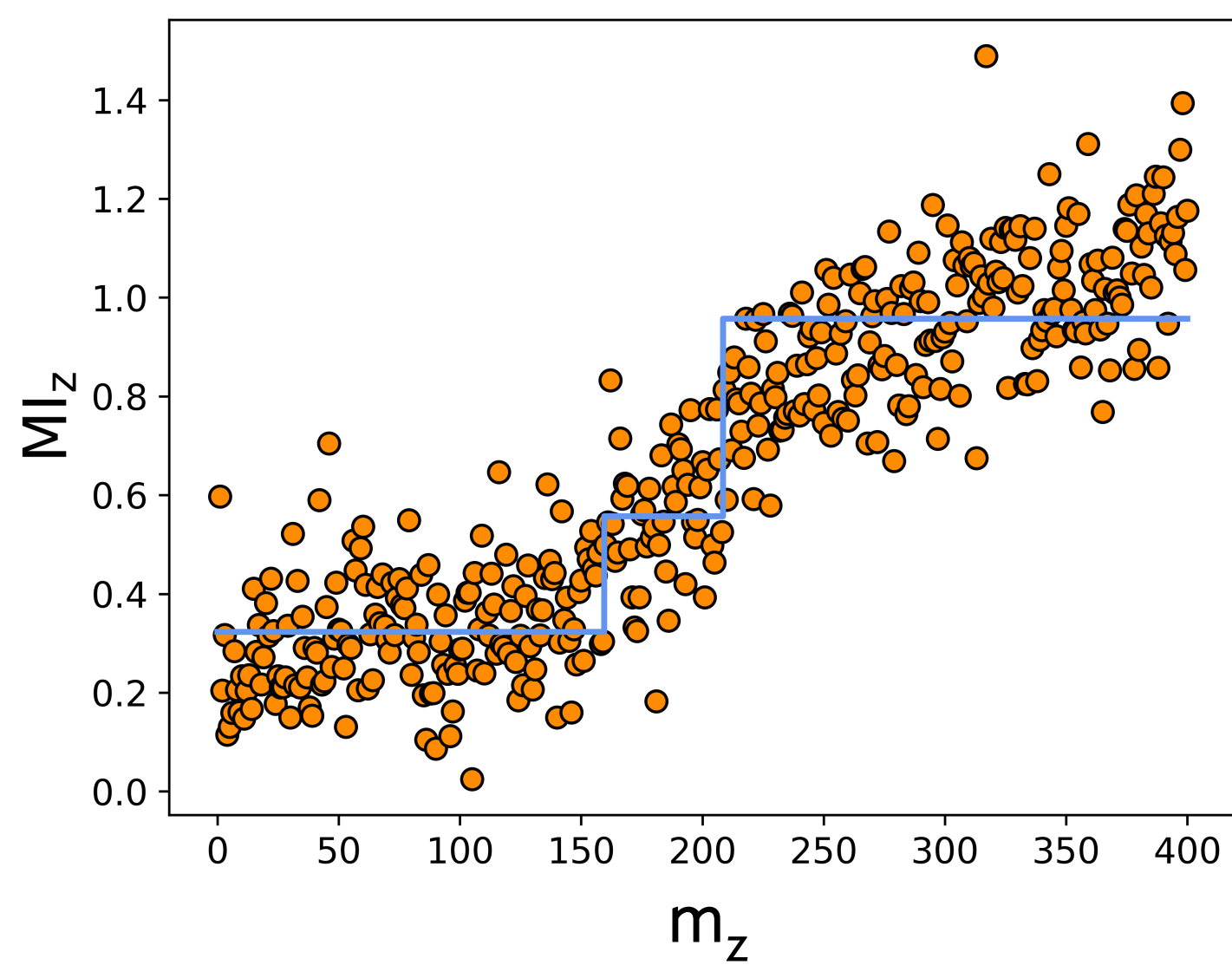




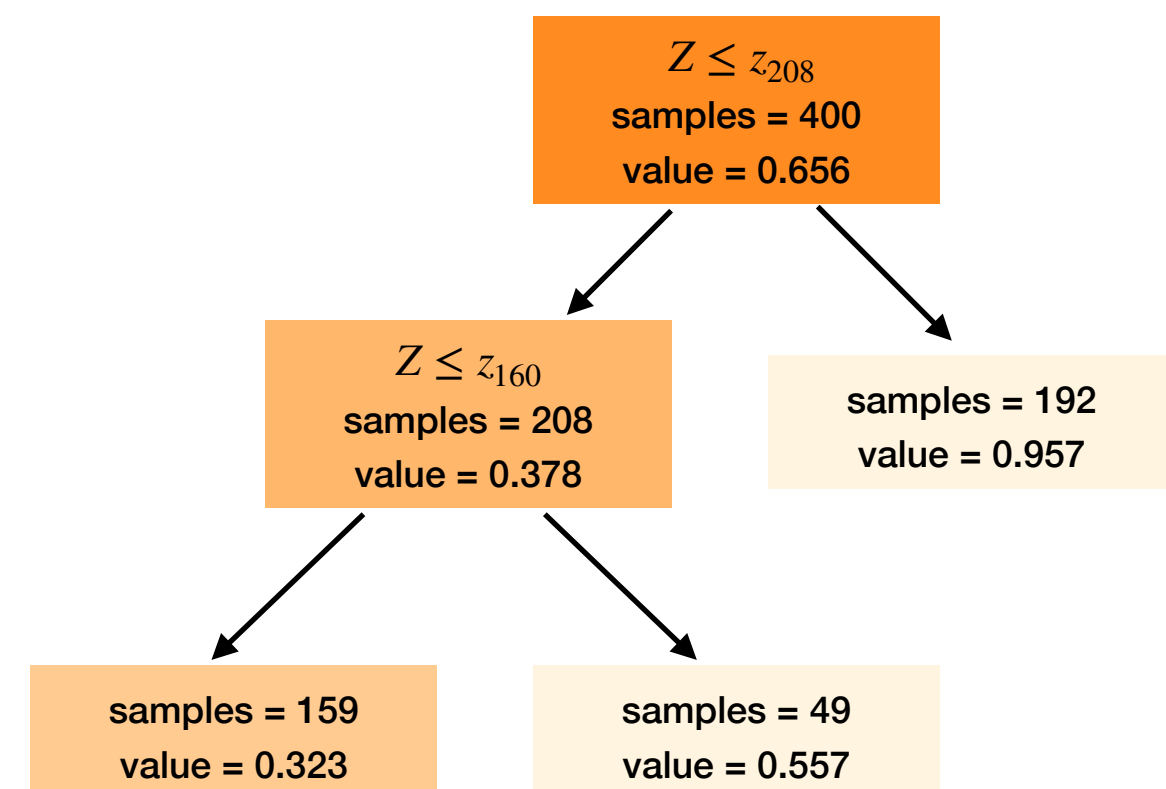
(a)



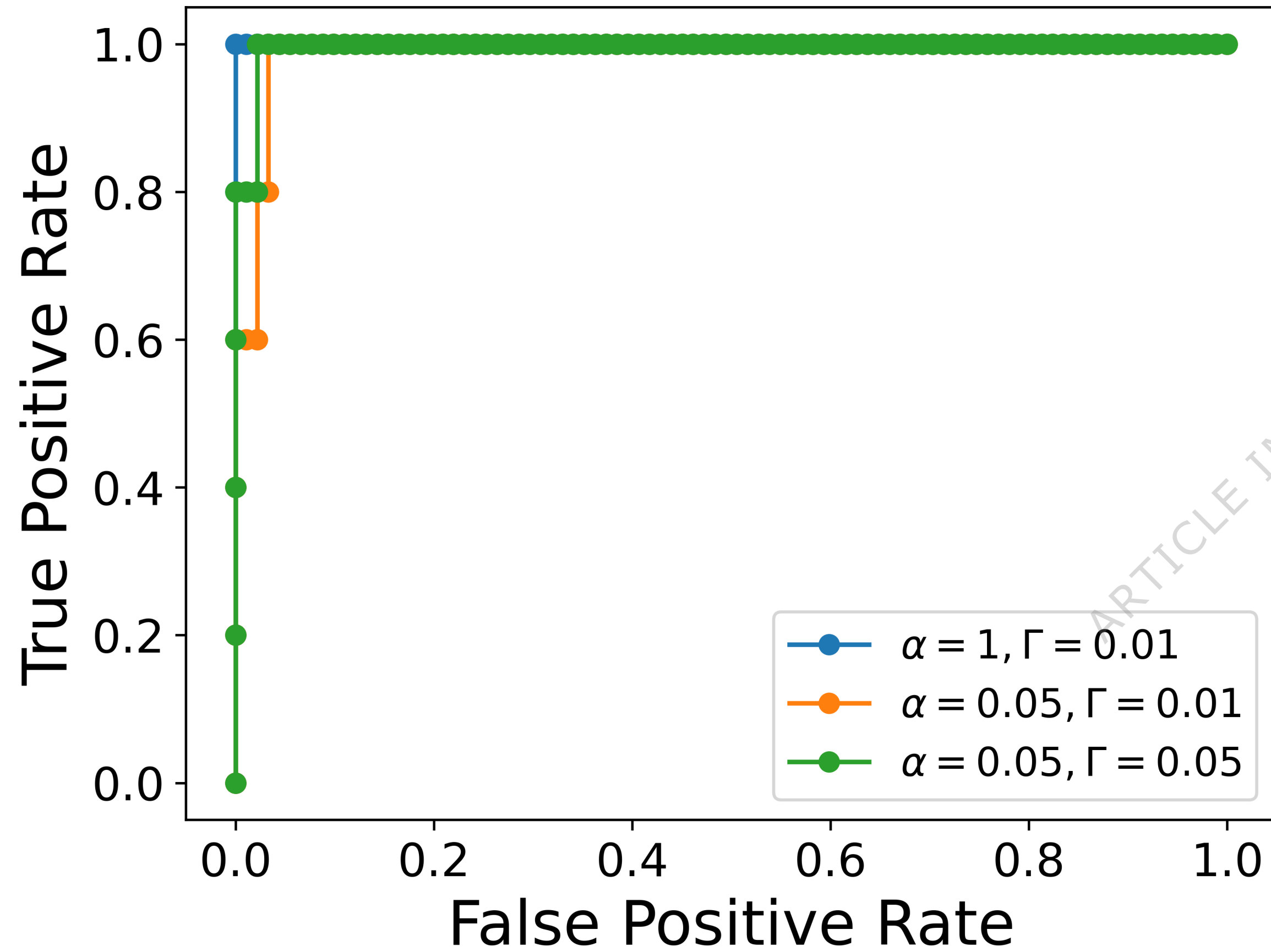
(b)



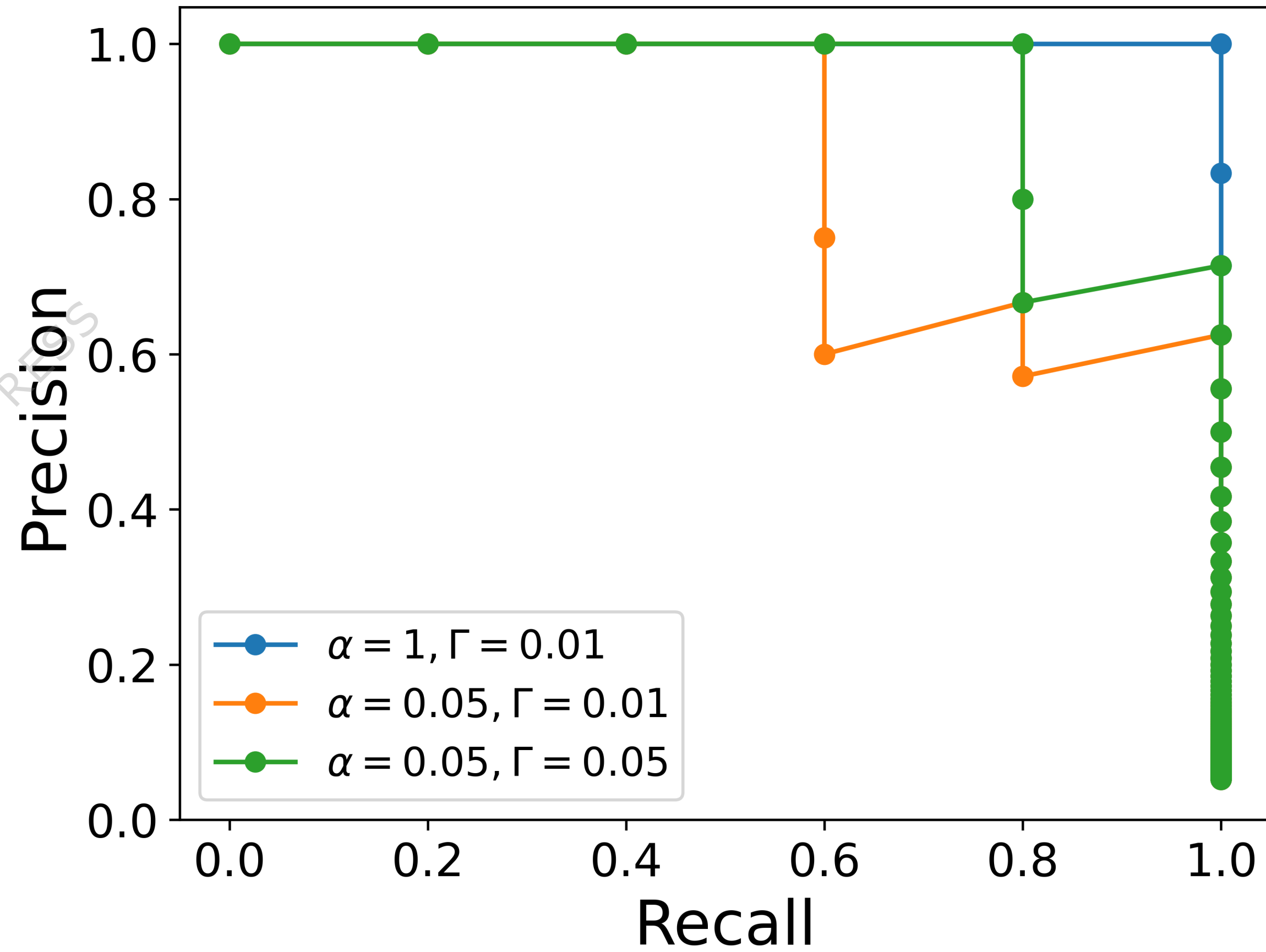
(c)



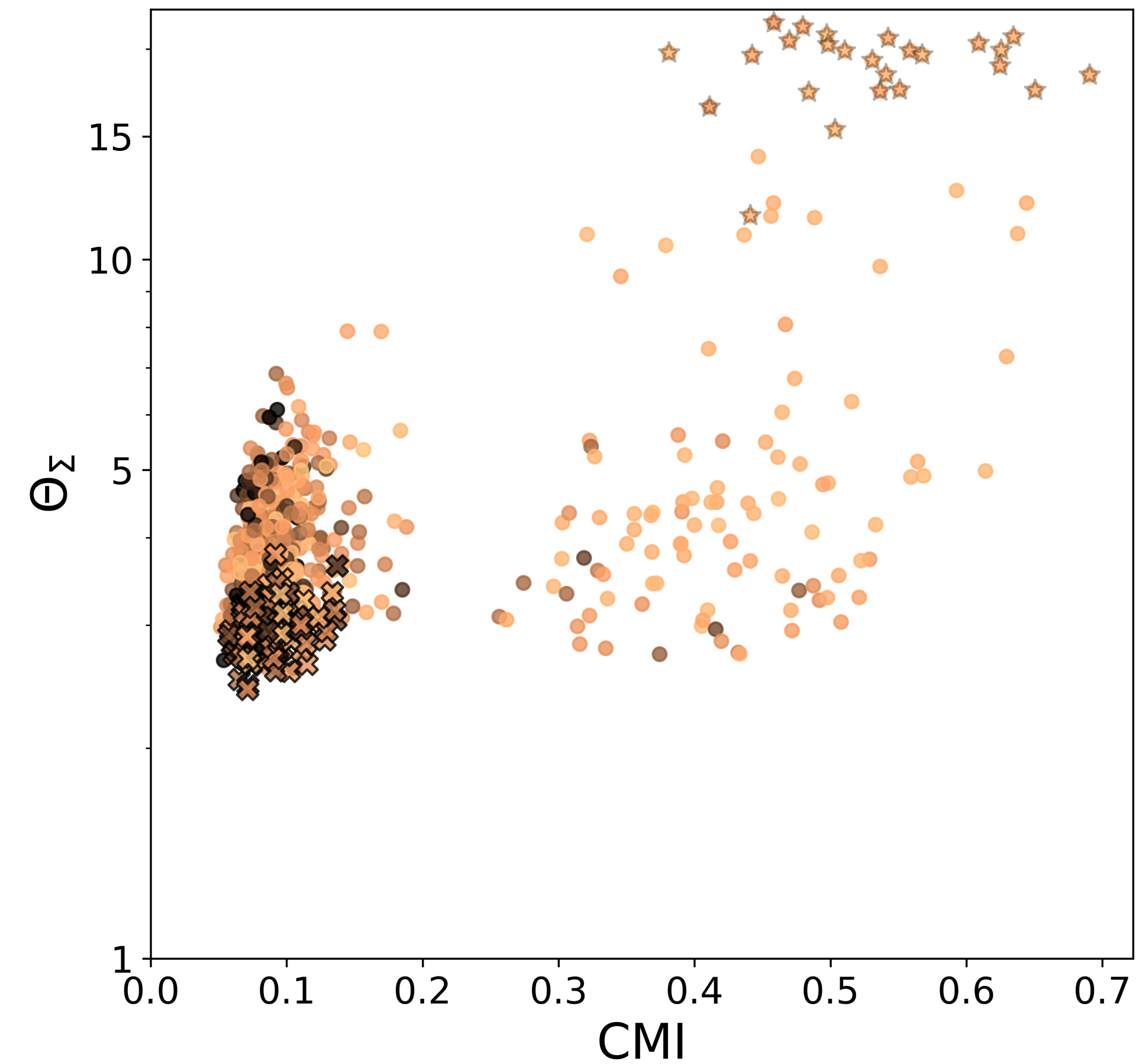
(a)



(b)

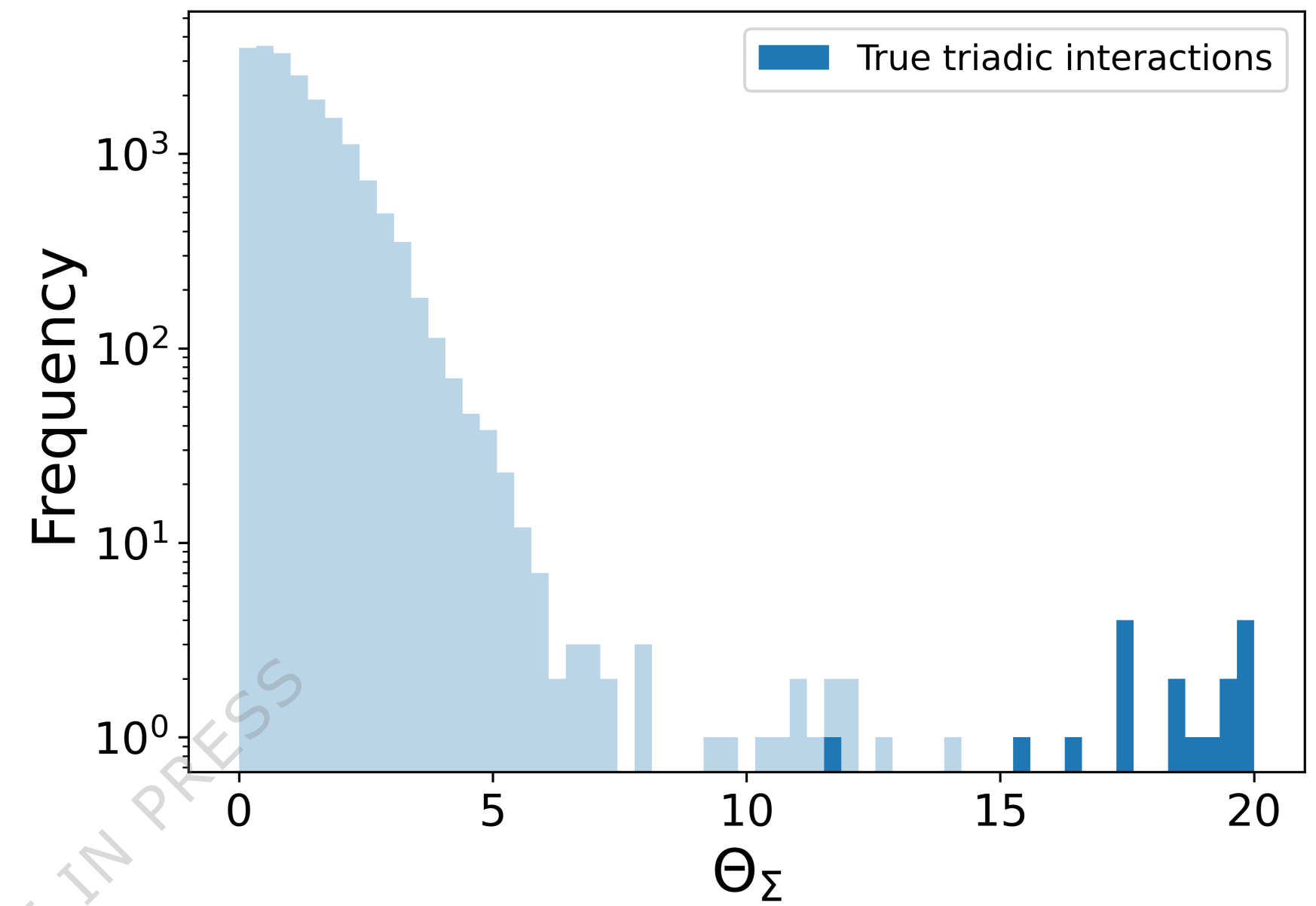


(a)



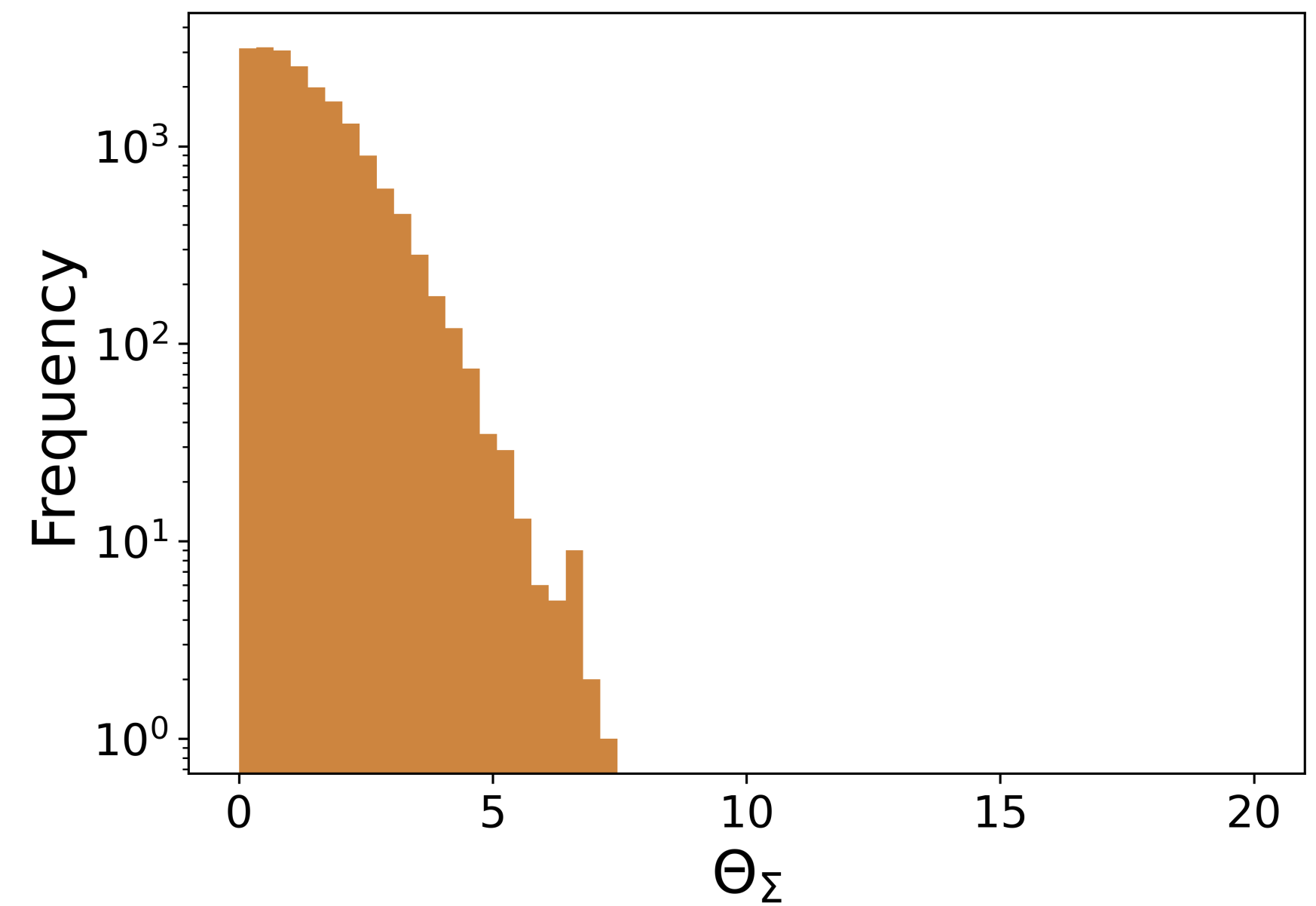
(b)

Network with triadic interactions

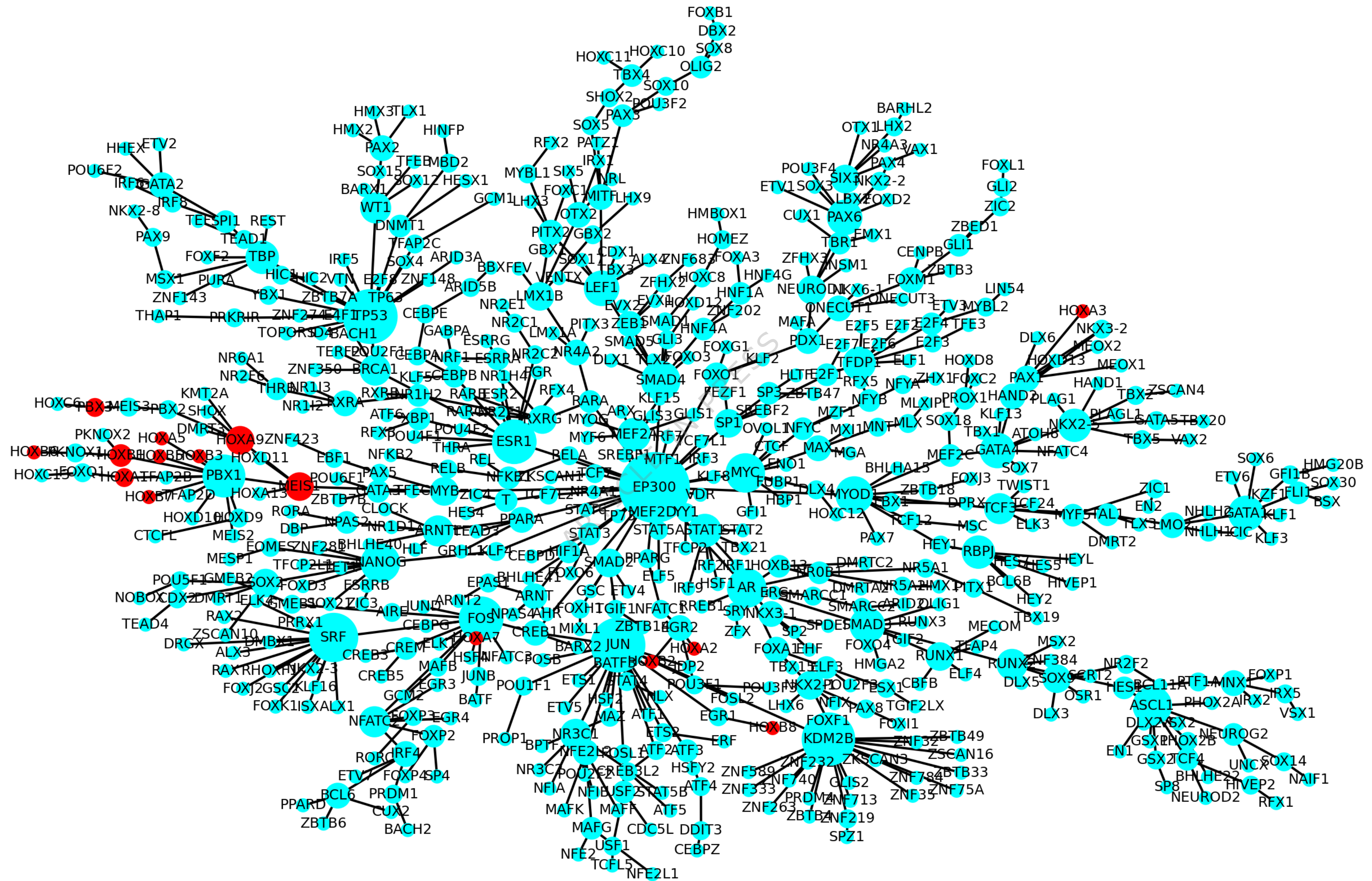


(c)

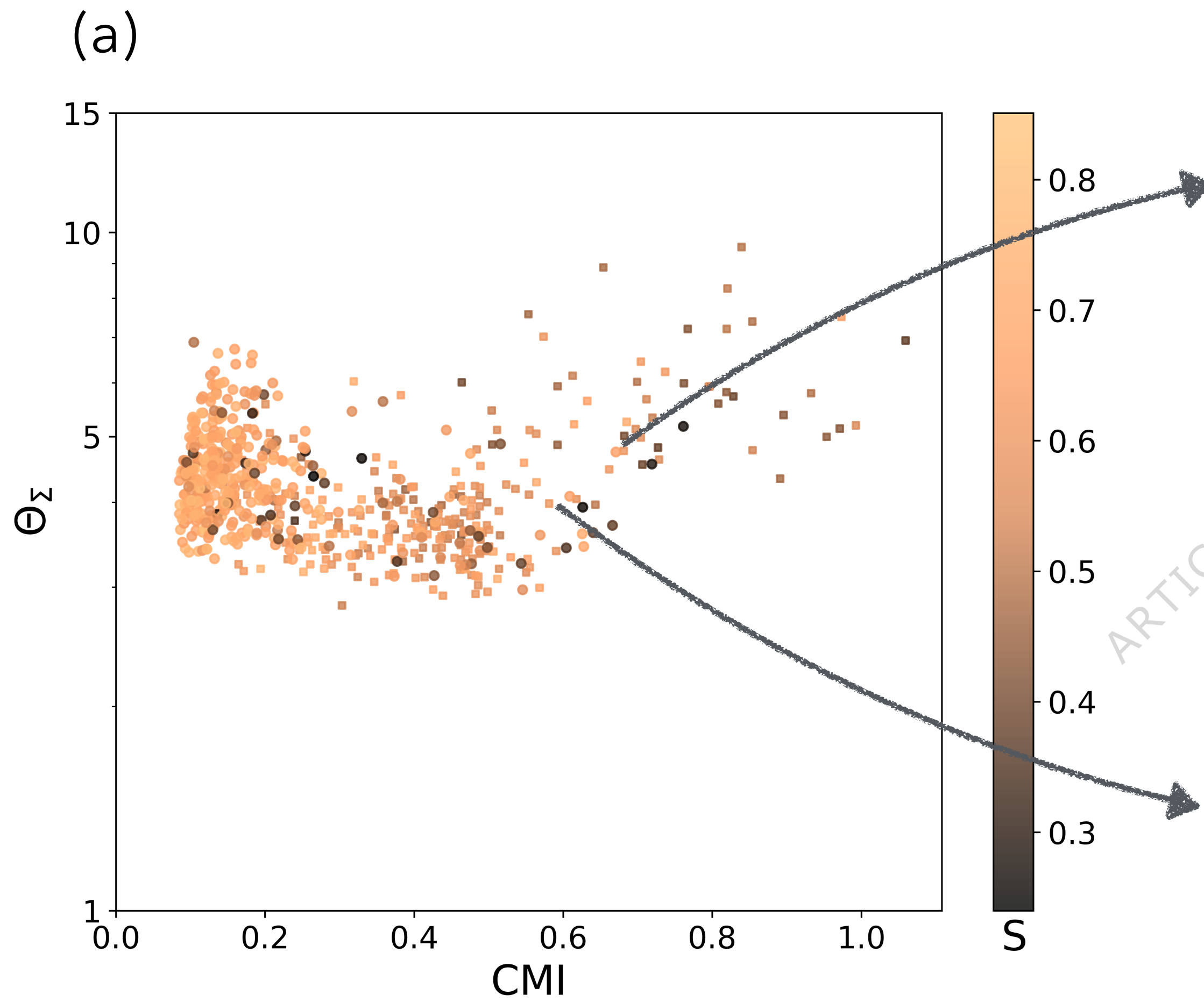
Network without triadic interactions



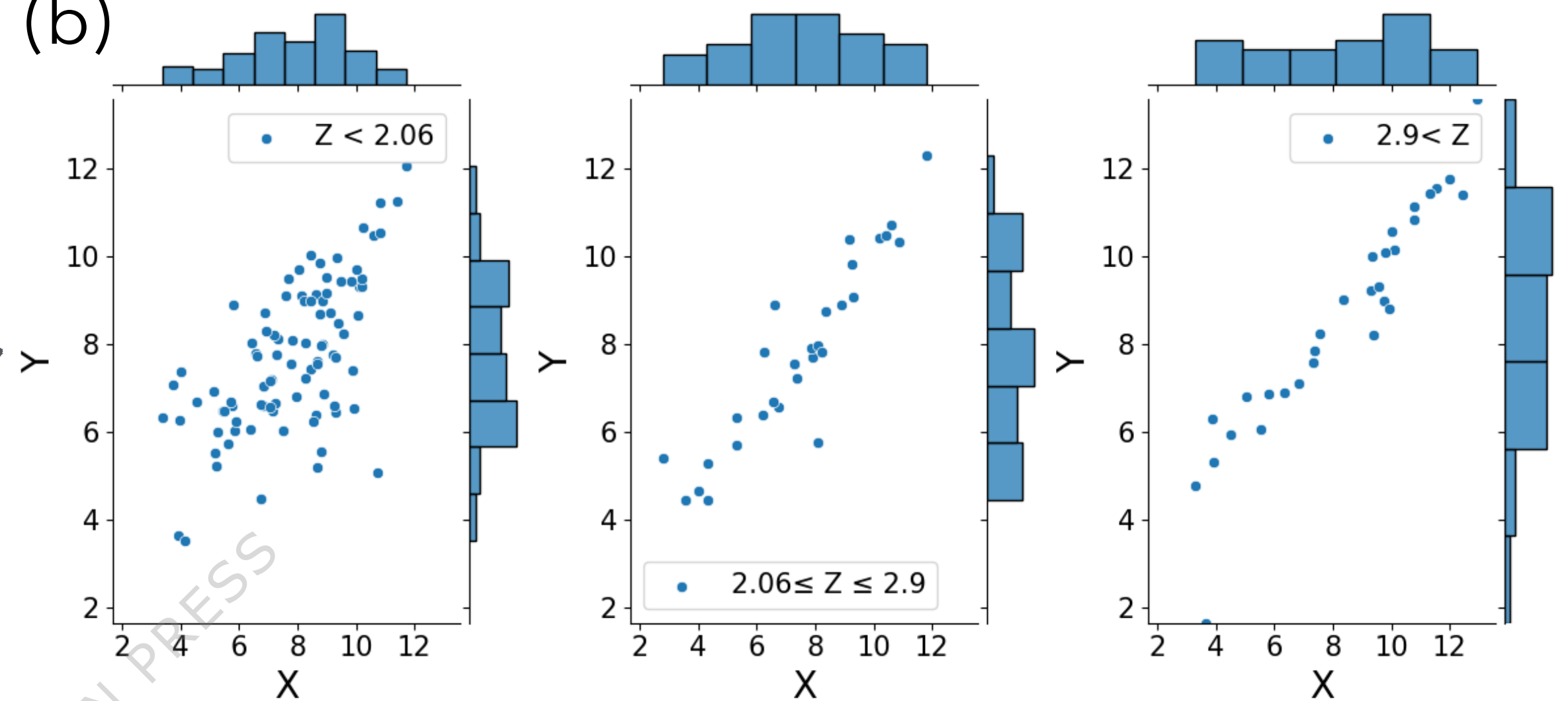




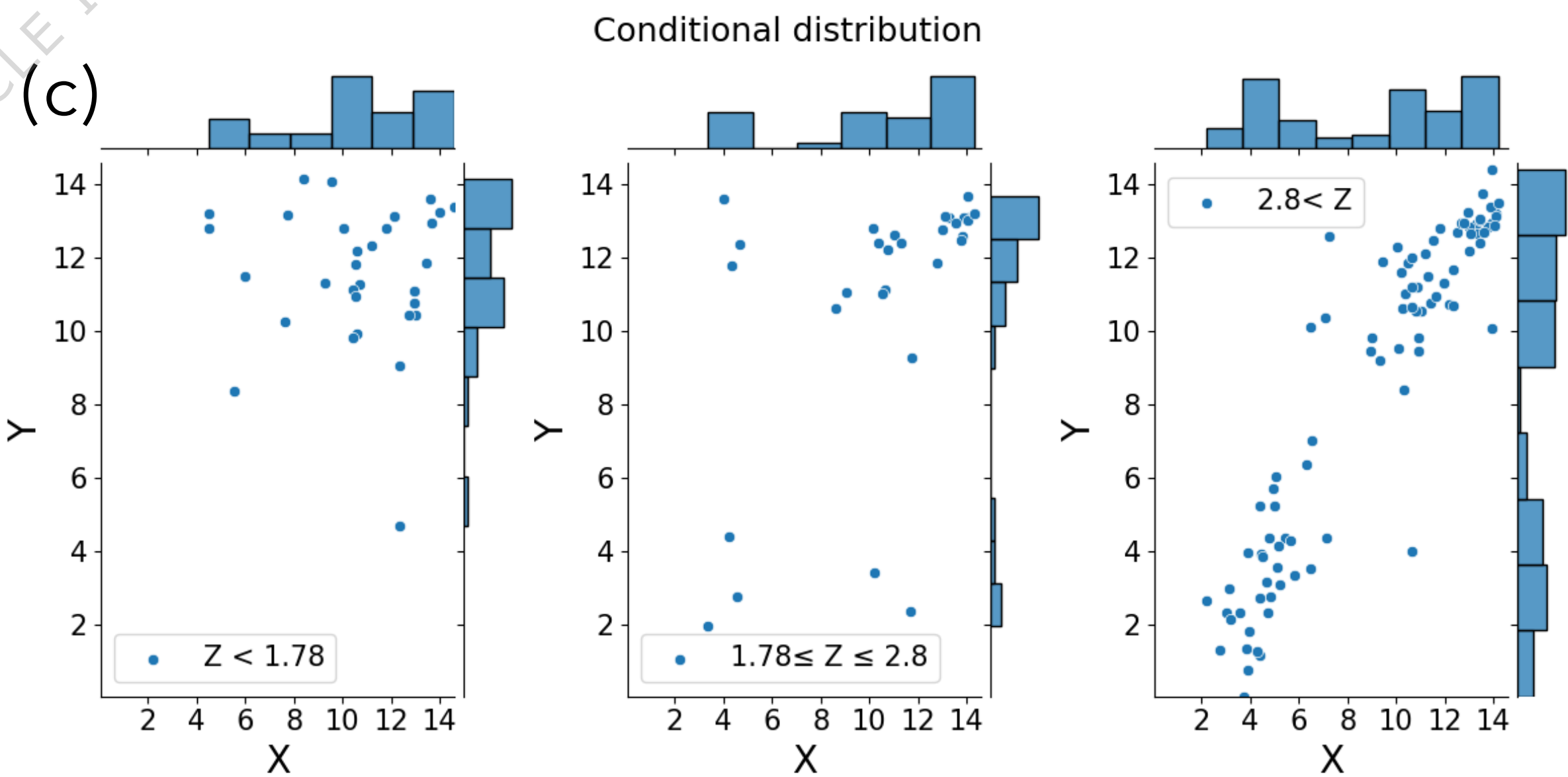




(b)



(c)





1 Triadic interactions, where one node regulates the interaction between two others, are a  
2 ubiquitous form of higher-order interaction. Here, the authors show that triadic interactions  
3 modulate mutual information between linked nodes and propose an algorithm to mine  
4 them in real biological data.

5

ARTICLE IN PRESS